Chapter 15

Deformable Organisms: An Artificial Life Framework for Automated Medical Image Analysis

Ghassan Hamarneh, Chris McIntosh, Tim McInerney, and Demetri Terzopoulos

Contents

We present an emerging, artificial life framework for medical image analysis. It was originally introduced as an extension to the established physics-based image segmentation approach known as *deformable models*. Although capable of extracting coherent, smooth boundaries from low-level image information, classical deformable models rely on human guidance to produce satisfactory segmentation results. Our artificial life approach augments the bottom-up, data-driven deformable model methodologies with top-down, intelligent deformation control mechanisms, yielding intelligent deformable models that we call *deformable organisms*. This is achieved by adding behavioral and cognitive modeling layers atop the physical and geometrical layers of the classical models. The resulting organisms evolve according to behaviors driven by decisions based on their perception of the image data as well as their internally encoded anatomical knowledge. Thus, deformable organisms are autonomous agents that can automatically segment, label, and quantitatively analyze anatomical structures of interest in medical images. This chapter motivates and overviews our novel framework, describes its fundamental principles, demonstrates prototype instances of deformable organisms, and summarizes recent advances.

15.1 Introduction

Medical imaging has become essential to the practice of medicine, but accurate, fully automatic medical image analysis (MIA) continues to be an elusive ideal. A substantial amount of knowledge is often available about anatomical structures of interest—characteristic shape, position, orientation, symmetry, associated landmarks, relationship to neighboring structures, and so on—in addition to plausible image intensity characteristics, subject to natural biological variability or pathological conditions. Even so, MIA researchers have not yet succeeded in developing completely automatic segmentation techniques that can take full advantage of such prior knowledge to achieve segmentation accuracy and repeatability. Although it may be generally acknowledged that such techniques will require the incorporation of context-based information within a robust decision-making framework (Duncan and Ayache, 2000), we contend that prior frameworks of this sort are inflexible and do not operate at an appropriate level of abstraction, which limits their potential to deal with the most difficult data sets.

Deformable models demonstrated early promise in image segmentation, and they have become one of the most intensively researched segmentation techniques (McInerney and Terzopoulos, 1996). They are curve, surface, or solid models that change shape or deform in order to fit to and thereby delineate (segment) target structures in medical images. The measure of

goodness of fit for deformable models is usually represented by an energy functional: the better the segmentation, the lower the energy. The dynamic, energy-minimizing deformations of these shape models are typically simulated numerically through the time integration of associated Euler-Lagrange partial differential equations derived using variational calculus. In addition, the classical deformable model methodology, which is epitomized by "snakes" (Kass et al., 1988), is also based on an interactive strategy that relies on human expert initialization and guidance.

The difficult challenge in automating this approach is to develop intelligent initialization mechanisms, including the setting of free parameters, along with control mechanisms that can guide the optimization-driven segmentation process. Researchers have tried in vain to obtain the right global behavior (i.e., on the scale of the entire image) by embedding nuggets of contextual knowledge into the low-level optimization engine. As a result of such efforts, it has become painfully obvious that current deformable models have little to no explicit "awareness" of where they are in the image, how their parts are arranged, or to what structures they or any neighboring deformable models are converging during the optimization process. To make progress toward full automation, we must augment the deformable model framework by combining the powerful low-level feature detection and integration component with intelligent high-level control components.

To this end, we have proposed a new approach to automated MIA that augments deformable model methodologies with concepts from the field of artificial life (ALife) (see Terzopoulos, 1999). Our ALife approach to MIA was originally introduced in Hamarneh, McInerney, and Terzopoulos (2001), Hamarneh (2001), and McInerney and others (2002). In particular, we developed deformable organisms, which are autonomous agents capable of automatically segmenting, labeling, and quantitatively analyzing anatomical structures of interest in medical images. By architecting deformable organisms in a bottom-up, layered manner, we can separate the global, model-fitting control functionality from the local feature detection and integration functionality; thus, the deformable organism can make decisions about the segmentation process at the proper conceptual level.

The result is autonomous and, to a degree, intelligent segmentation algorithms that are aware of their progress and apply prior knowledge in a deliberative manner during different phases of the segmentation process. Analogous to natural organisms capable of voluntary movement, the artificial organisms possess deformable bodies with distributed sensors, as well as (rudimentary) brains with motor, perception, behavior, and cognition centers. Deformable organisms are perceptually aware of the image analysis process (Figure 15.1). Their behaviors, which manifest themselves in proactive movement and alteration of body shape, are based on sensed image features, prestored anatomical knowledge, and a deliberate cognitive plan.

The layered architecture as well as the reusable behavior routines and other components facilitate the rapid implementation of powerful, custom-tailored

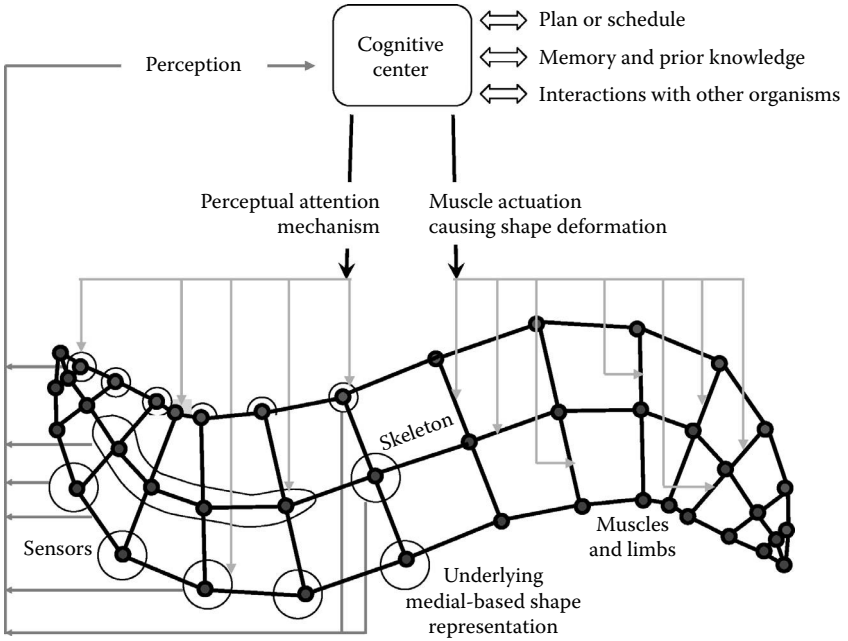

FIGURE 15.1: A deformable organism: the brain issues muscle actuation and perceptual attention commands. The organism deforms and senses image features whose characteristics are conveyed to the brain. The brain makes decisions based on sensory input, information in memory and prior knowledge, and a prestored plan, which may involve interaction with other organisms. (From Hamarneh, G., McInerney, T., Terzopoulos, D. 2001. In *Proceedings of the Medical Image Computing and Computer-Assisted Intervention*, Utrecht, the Netherlands, 66–75. With permission.)

deformable organisms that can serve as new tools for automated segmentation, object-based registration, and the quantification of shape variation.

The remainder of this chapter is organized as follows. We begin with an overview of deformable organisms (Section 15.2) and present two illustrative examples. Following a detailed motivation and background, we review the ALife modeling framework, outline the notion of controlled deformations, and explain how intelligent decision and control mechanisms are incorporated into deformable organisms. The different layers of deformable organisms architecture are explained in Section 15.3. Recent research advances that utilize this framework, including extensions to 3-D physics-based deformations, vessel and spinal crawlers, evolutionary models, and an Insight Users Toolkit (ITK)-based deformable organisms software framework, are presented in Section 15.4. Examples and results are presented throughout the chapter.

15.2 Background and Related Work

Deformable organisms are deformable models equipped with higher-level control algorithms motivated by artificial life. The latter are responsible for controlling the shape deformations in a systematic manner based on a set of relevant criteria, a predefined set of situationally dependent actions, and the current system state, including the image and even the user.

15.2.1 Illustrative examples of deformable organisms

Several prototype deformable organisms based on an axis-symmetric body morphology were presented by McInerney and colleagues (2002). This geometric representation in conjunction with a set of multiscale deformation operators affords the motor center in the brain of the organism precise local growth and shape control processes at a variety of scales. Various reusable behavior routines, which support single organism behaviors as well as multiple, interacting organism behaviors, were also examined. Interaction among organisms may be as simple as (a) collision detection and the imposition of nonpenetration constraints between two or more organisms in contact; (b) one or more parent organisms spawning a new child organism and supplying it with appropriate initial conditions; or (c) the sharing of statistical shape constraints and/or image appearance information between organisms. More complex, rule-based interactions are also possible.

Figure 15.2 illustrates deformable organisms with a nontrivial example involving the detection and detailed segmentation of the lateral ventricle, caudate nucleus, and putamen in the left and right halves of a transverse 2-D MR image of the brain. Since the ventricles are the most discernible and stable structures in this imaging modality, the segmentation process begins with the release of two "ventricle organisms" in the black background region outside the cranium, at the upper left and right edges of the image in subfigure (1). Performing a coordinated scanning behavior, the organisms proceed first to locate the tops of the ventricles, as shown in the zoomed-in view of subfigure (2), and their inner and outer (with respect to the brain) boundaries (3)–(5). Next, both ends of each ventricle organism actively stretch to locate the upper and lower lobes of the ventricle (6), and then the organism fattens to finish segmenting the ventricle (7). Each organism employs the information that it has gleaned about the shape and location of the segmented ventricles to spawn and initialize a caudate nucleus organism in an appropriate location (8). Each caudate nucleus organism first stretches to locate the upper and lower limits of the caudate nucleus (9) then fattens until it has accurately segmented the caudate nucleus (10). From its bottommost point in the image, each caudate nucleus organism then spawns and initializes a putamen organism (11), which then moves laterally outward toward the low-contrast putamen (12). Each putamen organism then rotates and bends to latch onto the nearer

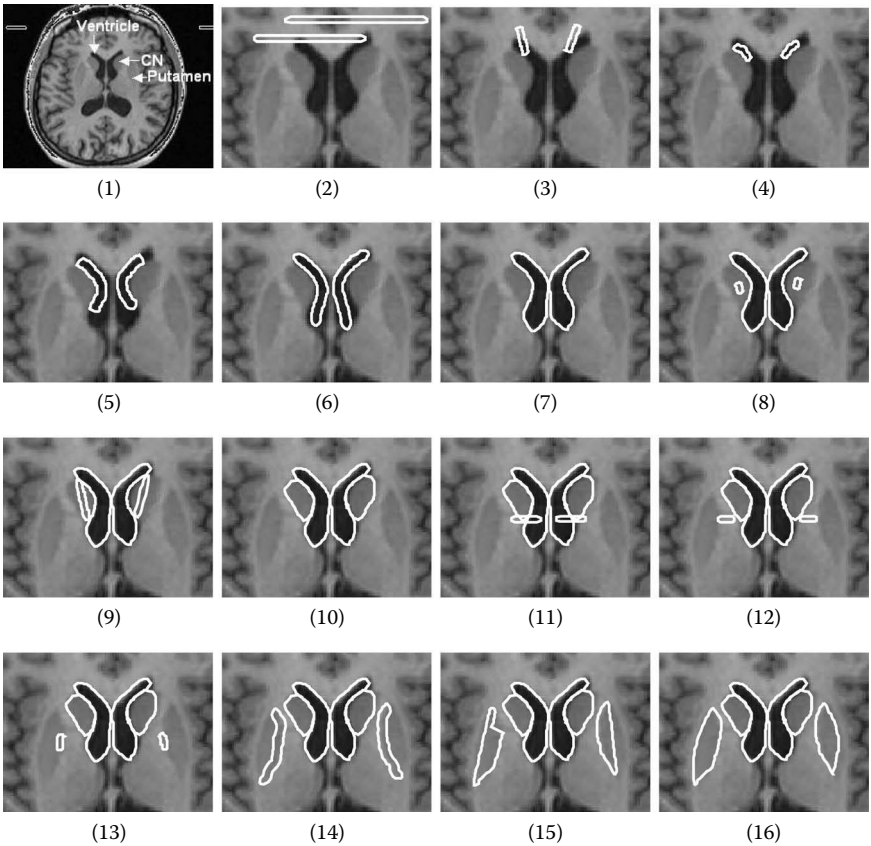

FIGURE 15.2: Automatic brain MR image segmentation by multiple deformable organisms. The sequence of images illustrates the temporal progression of the segmentation process. Deformable lateral ventricle (1–7), caudate nucleus (8–10), and putamen (11–16) organisms are spawned in succession and progress through a series of behaviors to detect, localize, and segment the corresponding structures in the MR image (see text). (From McInerney, T., Hamarneh, G., Shenton, M., Terzopoulos, D. 2002. *Medical Image Analysis*, 6(3): 251–266. With permission.)

putamen boundary (13). Next, it stretches and grows along the boundary until it reaches the upper and lower ends of the putamen (14), thus identifying the medial axis of the putamen (15). Since the edges of the putamen boundary near the gray matter are often weak, the organism activates an explicit search for an arc (parameterized by a single curvature parameter) that best fits the low-contrast intensity variation in that region, thus completing the segmentation (16).

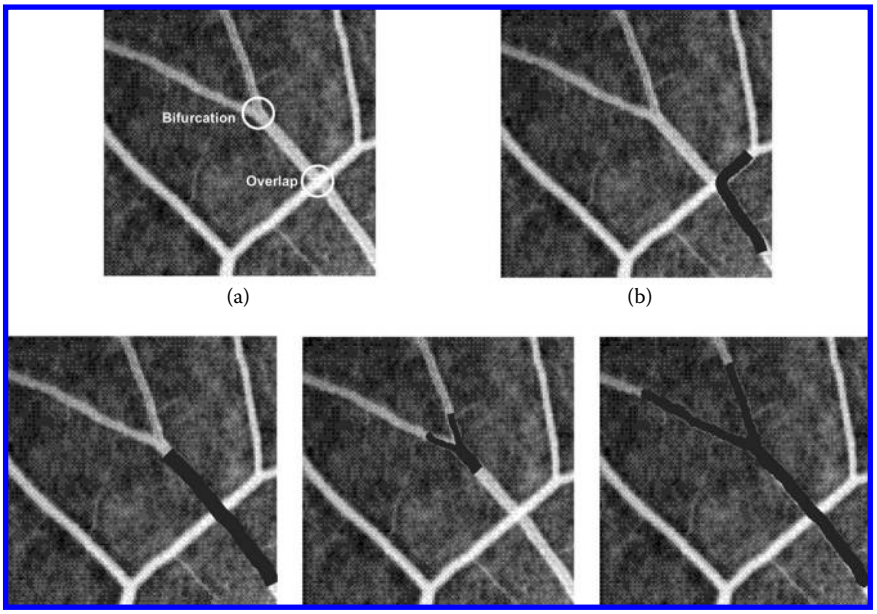

FIGURE 15.3: Multiple deformable organisms segmenting vascular structures in an angiogram. (a) Vessel overlap and bifurcation. (b) A simplistic vessel organism incorrectly bends into the more prominent overlapping vessel. (c) Appropriate high-level behaviors enable the vessel organism to identify the overlap and distinguish it from bifurcations. (d) Upon identifying a bifurcation, the organism spawns two new organisms, each of which proceeds along a branch. (e) The segmented vessel and branches. (From McInerney, T., Hamarneh, G., Shenton, M., Terzopoulos, D. 2002. *Medical Image Analysis*, 6(3): 251–266. With permission.)

As a second illustrative example, Figure 15.3 shows a different type of axis-symmetric deformable organism specialized to ribbonlike structures. This organism, called a vessel crawler, segments a vascular structure in a retinal angiogram. If given insufficient prior knowledge, the organism can latch onto the wrong overlapping vessel as shown in Figure 15.3b. However, given a suitable repertoire of perceptual capabilities and behavior routines (see Sections 15.3.3 and 15.3.4), the vessel organism can distinguish between overlapping vessels and deal with bifurcations (Figure 15.3c). When a bifurcation is encountered, the organism spawns two new child vessel organisms (Figure 15.3d), each of which extends along a branch (Figure 15.3e). These 2-D vessel crawlers can be extended to 3-D (Section 15.4.3).

15.2.2 Motivation and background

Current model-based MIA frameworks utilize geometric and often physical modeling layers. The models are fitted to images by minimizing energy functions, simulating dynamical systems, or applying probabilistic inference methods, but they do not control this optimization process other than in primitive ways, such as monitoring convergence or equilibrium. Some deformable models incorporate prior information to constrain shape and image appearance and the observed statistical variation of these quantities (Cootes et al., 1995; Cootes et al., 1999; Szekely et al., 1996). These models have no explicit awareness of where they or their parts are, and therefore the effectiveness of such constraints is dependent on appropriate model initialization. The lack of self-awareness may also prevent models from knowing when to trust the image feature information and ignore the prior constraint information or vice versa. The lack of optimization control can prevent these models from performing intelligent searches over their parameter spaces during the fitting process; that is, the constraint information is applied more or less indiscriminately and, once set in motion, the optimization process continues "mechanically" to completion.

Furthermore, because there typically is no active, deliberate search for stable image features, the models can latch onto nearby spurious features (Cootes et al., 1999). Their short-sighted decision-making abilities prevent these models from correcting missteps. Even if global optimization methods such as simulated annealing are employed to perform more extensive searches, the parameter space of the model is explored in a rather random fashion and there is no guarantee (other than an excruciatingly slow, asymptotic one) that the correct solution will be found. Moreover, it remains an open question whether suitable solution metrics can be defined for many MIA tasks using the "language" of objective functions and low-level optimization, or even of probabilistic inference.

There are several examples of earlier MIA systems that attempt to leverage top-down reasoning strategies against bottom-up feature detection, usually with limited success (e.g., the ALVEN cardiac left ventricular wall motion analyzer; Tsotsos et al., 1980). Other notable related work is the "visual routines" theory of Ullman (1984), which was proposed as a model of intermediate visual perception and includes a prominent top-down, sequential control mechanism. More recently, researchers have attempted to add some model-fitting control capability by constructing hierarchical deformable model-based systems (McInerney and Kikinis, 1998; Shen and Davatzikos, 2000). The idea here is that it is often possible to prioritize the strength or stability of different image features of the target structure(s). These systems attempt to control the fitting process such that the models systematically shift their focus from stable image features to less stable features. However, features may occur at different locations and scales and may vary from low-level landmark points to curves or surface patches to volumetric regions or to more complex features. Without

a proper nomenclature with which to define the high level features, and a system organization that provides more complete and easily programmable control over the model, it may be difficult to exploit this information effectively.

Alternatively, if a model can be made aware of itself and its environment, it can potentially be programmed to perform a more intelligent search for correct solutions by exploiting global contextual knowledge more effectively. For example, it may explore several alternative paths and choose the optimal result. To add this ability to deformable models, it seems prudent to investigate analogies with living systems.

15.2.3 Artificial life modeling

The modeling and simulation of living systems is central to an emerging scientific discipline known as artificial life (ALife).* In recent years, the ALife paradigm has had substantial impact in computer graphics, giving impetus to several important avenues of research and development, including artificial plants and animals, behavioral modeling and animation, and evolutionary modeling (Terzopoulos, 1999). These graphical models typically employ geometry- and physics-based techniques, as is characteristic of the deformable models used in MIA, but they also aspire to simulate many of the biological processes that characterize living systems—including birth and death, growth and development, natural selection, evolution, perception, locomotion, manipulation, adaptive behavior, learning, and cognition.

Most relevant to the MIA approach presented in this chapter is the ALife modeling of animals. The key components of artificial animals such as the prototypical "artificial fishes" (Terzopoulos et al., 1994) are synthetic bodies, including functional motor organs (contractile muscles), sensory organs (eyes, etc.), and most importantly, brains with motor, perception, behavior, and learning centers. In the motor center, motor controllers coordinate muscle actions to carry out specific motor functions, such as locomotion and sensor control. The perception center incorporates perceptual attention mechanisms, which support active perception that acquires information about the dynamic environment. The behavior center realizes an adaptive sensorimotor system through a repertoire of behavior routines that couple perception to action. The learning center in the brain enables the artificial animal to learn motor control and behavior through practice and sensory reinforcement.

To manage the complexity, artificial animals are best organized hierarchically, with each successive modeling layer adding to the more basic functionalities of underlying layers (Terzopoulos, 1999). At the base of the modeling

*See Levy (1992) for an entertaining perspective of the genesis of the artificial life field. Journals such as *Artificial Life* and *Adaptive Behavior* chronicle the state of the art.

hierarchy, a geometric modeling layer represents the morphology of the animal. Next, a physical modeling layer incorporates biomechanical principles to constrain geometry and emulate biological tissues. Further up the hierarchy, a motor control layer motivates internal muscle actuators to synthesize lifelike locomotion. Behavioral and perceptual modeling layers cooperate to support a reactive behavioral repertoire. The apex of the modeling pyramid, the domain of classical artificial intelligence, simulates the proactive or deliberative abilities of higher animals. Here, a cognitive modeling layer concerns how knowledge is represented and how automated reasoning and planning processes achieve high-level goals.

15.2.4 Controlling shape deformation

Top-down, knowledge-driven, model-fitting strategies require underlying shape representations that are responsive to high-level controlled shape deformation commands. As the organism's cognitive layer selects a behavior, the activated behavior routine will execute a series of shape deformations realized through high-level motor programs, which in turn are realized through simpler low-level motor skills. The goal here is to intelligently control the different types and extent of model deformations during the model-fitting process, focusing on the extraction of the most stable image features before proceeding to object regions with less well-defined features.

The choice of shape representation is undeniably crucial for segmentation, recognition, and interpretation of medical images. The study of shape has attracted a great deal of attention within the medical image analysis community (Bookstein, 1997; Costa and Cesar, 2000; Dryden and Mardia, 1998). A desirable characteristic in a shape representation is the ability to easily specify nonrigid object deformations at multiple locations and scales. Deformable shape models (McInerney and Terzopoulos, 1996), in particular, are mostly boundary based, and therefore multiscale deformation control is constructed from low-level boundary point sets and not upon object-relative geometry. Although they provide excellent local shape control, they lack the ability to undergo intuitive global deformation and to decompose shape variability into intuitive deformations, with some notable exceptions (Terzopoulos and Metaxas, 1991). It is therefore difficult to incorporate intelligent deformation control at the right level of abstraction into the conventional deformable model framework. Consequently, deformable models remain sensitive to initial conditions and spurious image features in image interpretation tasks. Hierarchical boundary-based shape models (Lachaud and Montanvert, 1999; Mandal et al., 1998; Miller et al., 1991; Montagnat and Delingette, 1997) and parameterized, free-form, and volumetric deformation mechanisms have been proposed (Barr, 1984; Coquillart, 1990; Sederberg and Parry, 1986; Singh and Fiume, 1998). They are also typically not defined in terms of the object; rather, the object is unnaturally defined in terms of the representation or deformation mechanism. Other 3-D shape representations

with similar drawbacks include spherical harmonics, finite element models, nonuniform rational B-splines, and wavelet-based representations (Burel and Henocq, 1995; Davatzikos et al., 2003; McInerney and Terzopoulos, 1995; Mortenson, 1997).

Shape models founded upon the use of the medial-axis transform (Blum, 1973) are a powerful alternative to boundary-based and volume-based techniques (Attali and Montanvert, 1997; Borgefors et al., 1999; Bouix et al., 2000; Dimitrov et al., 2003; Fritsch et al., 1997; Hamarneh and McInerney, 2003; Hamarneh et al., 2004; Leymarie and Levine, 1992; Pizer and Fritsch, 1999; Pizer et al., 2003; Sebastian et al., 2001; Siddiqi et al., 2002; Hamarneh et al., 2007). Medial representations provide both a local and global description of shape. Deformations defined in terms of a medial axis are natural and intuitive and they can be limited to a particular scale and location along the axis, while inherently handling smoothness and continuity constraints.

Statistical models of shape variability have been used for medical image interpretation (Cootes et al., 1995; Cootes et al., 2001; Duta et al., 1999; Leventon et al., 2000; Szekely et al., 1996). These typically rely on principal component analysis (PCA) and hence are only capable of capturing global shape variation modes (Cootes et al., 1995). This is because the eigen decomposition is typically performed on the covariance matrix of all the landmark locations representing the shape, without any spatial localization, as opposed to performing location- and deformation-specific dimensionality reduction (Hamarneh et al., 2004). The statistical analysis of medial-axis-based shape representation has been the focus of recent research (Fletcher et al., 2004; Grenander, 1963; Lu et al., 2003; Styner et al., 2003; Yushkevich et al., 2003).

15.2.5 Intelligent decision and control

The layered architecture enables a deformable organism to perform intelligent searches for anatomical features in images by allowing it to make appropriate high-level deformation decisions. The higher control layers afford the organism a nontrivial "awareness" (i.e., it knows where it is, where its parts are, and what it is seeking) and therefore it is more effectively able to utilize global contextual knowledge of the target anatomical structure, as well as local knowledge of the anatomical feature on which it is currently focused.

An organism typically begins by searching for the most stable anatomical features in the image, and then proceeds to the next best features, and so on. Alternatively, an organism may interact with other organisms to determine optimal initial conditions or resolve conflicting views of data. Once stable features are found and labeled, an organism can selectively use prior knowledge in regions known to offer little or no feature information. That is, the organism intelligently "fills in" the boundary in ways tailored to specific regions of interest in the target structure.

A deformable organism's awareness allows it to perform smart, flexible feature searches. It need not be satisfied with the nearest matching feature, but can look further within a region to find the best match, thereby avoiding globally suboptimal solutions. Furthermore, by carrying out explicit searches for features, correct correspondences between the organism and the data are more readily assured. If an expected feature cannot be found, an organism may "flag" the anomaly. If multiple plans exist, another plan can be selected and/or the search for the missing feature postponed until further information is available (e.g., from a neighboring organism). Alternatively, the organism can retrace its steps and return to a known state, and then inform the user of the failure. A human expert can intervene and put the organism back on course by manually identifying the feature. This strategy is possible because of the sequential and spatially localized nature of the deformable organism fitting process.

To support intelligent feature search, an organism needs powerful, flexible and intuitive model deformation control coupled with a flexible feature perception system. We currently achieve this with a set of "motor" (i.e., deformation) controllers and medial-axis-based deformation operators. Deformation controllers are parameterized procedures dedicated to carrying out a complex deformation function, such as successively bending a portion of the organism over some range of angle or stretching part of the organism forward some distance. They translate natural control parameters such as ⟨bend-angle; location; scale⟩ or ⟨stretch-length; location; scale⟩ into detailed deformations. The first deformable organisms used medial-profiles (Hamarneh et al., 2004) for their shape representation, which follow the geometry of the structure and describe general and intuitive shape variation (stretch, bend, thickness). Shape deformations result from the application on the medial profiles of deformation operators at certain locations and scales, or by varying the weights of the main variation modes obtained from a hierarchical (multiscale) and regional (multilocation) principal component analysis of the profiles (Hamarneh et al., 2004). Section 15.3 describes these organism components in detail.

Finally, an organism may begin in an "embryonic" state with a simple protoshape, and then undergo controlled growth as it develops into an "adult," proceeding from one stable object feature to the next. Alternatively, an organism may begin in a fully developed state and undergo controlled deformations as it carries out its model-fitting plan. The evolutionary corpus callosum organisms (Section 15.4.5) are an example of the latter.

Which type of organism to use, or whether to use some sort of hybrid organism, is dependent on the image and shape characteristics of the target anatomical structure. In summary, the ALife modeling paradigm provides a general and robust framework within which standard behavior subroutines may be employed to build powerful and flexible custom-tailored deformable organisms.

15.3 Deformable Organism Architecture

This section describes the layers of the deformable organism architecture, starting with the lowest layers (geometrical and physical) and working up to the higher layers (sensory, behavioral, and cognitive).

15.3.1 Geometrical layer (morphology and topology)

The geometrical layer of the deformable organism defines the shape representation as well as the morphological and topological constraints of the organism. The deformable organisms developed to date are based on medial-axis (Hamarneh et al., 2004) or medial-sheet (Hamarneh et al., 2007) deformable shape representations (Figure 15.1). The medial shape representation allows for a variety of intuitive and controlled shape changes that are described relative to the natural geometry of the object rather than as local displacements to its boundary. These changes in shape include stretching, thickening, or bending and are realized either as purely geometric deformations* or as deformations simulated at the physics layer of the organism (Hamarneh and McInerney, 2003; Hamarneh and McIntosh, 2005).

For example, medial profiles were used in the lateral ventricle, caudate nucleus, and putamen organisms, 2-D vessel crawler (Section 15.2.1), the corpus callosum (CC) organism (Section 15.3.4), and in the "evolutionary CC organism" (Section 15.4.5). Medial profiles are a set of functions that describe the geometry of the structure through general, intuitive, and independent shape measures (length, orientation, and thickness) taken with respect to the medial axis (Hamarneh et al., 2004). For instance, the thickness profile describes the distance from the medial axis to the boundary, while the orientation profile describes the angular offset between sequential medial nodes. In the physics-based CC organism (Section 15.4.1), the underlying geometry is a medial mesh of vertices and edges that is automatically constructed from the pruned skeletons of a training set of shapes (Hamarneh and McInerney, 2003). In 3-D vessel and spinal crawlers (Sections 15.4.3 and 15.4.4), the geometry is a tubular mesh with an underlying medial axis and a radial thickness measure connecting to a triangulated surface. The chosen representation imposes a strong tubular shape prior, while remaining general enough to allow for arbitrary stretching, bending, thickening, and branching, which is suitable for accurately representing tubular structures and complex vascular networks.

In the ITK Deformable Organisms software framework (Section 15.4.6), the developer of new deformable organism instantiations can substitute

*Deformations that manipulate the geometry of the model directly and without physical constraint.

various geometrical C++ classes, which conform to the predefined interfaces of abstract base classes. This restriction ensures that the user can employ different geometric layers (different shape parameterizations) while retaining all of the framework's most general abilities—those that are not specific to a particular parameterization. For example, the system can change between (Lagrangian) mesh models that explicitly store the locations of the surface and medial nodes or implicit (Eulerian) shape models, where the shape is the zero level-set of an embedding function.

15.3.2 Physical layer (motor system and deformations)

The physical layer of a deformable organism is analogous to the muscles in the human body. The actions carried out by the physical layer of the organism are divided into two classes: deformations and locomotions. The deformation capabilities of the organism constitute its low-level motor skills or basic actuations. These include global deformations such as affine transformations or localized (nonlinear) deformations such as a simple bulge or stretch. The more complex locomotion actions are the high-level motor skills of the organism. They result from several basic motor skills, which are parameterized procedures that carry out complex deformation functions, such as sweeping over a range of rigid transformation (translation, rotation) parameters; sweeping over a range of stretch, bend, or thickness parameters; bending at increasing scales; and moving a bulge along the boundary. Other high-level deformation capabilities include smoothing the medial axis or the boundary of the model, or reinitializing the medial axis to a position midway between the boundaries on both sides of the medial axis (sheet). See Figure 15.4 for examples.

Clearly the implementation of these deformations depends on the underlying geometry. Deformable organisms based on medial profiles can be deformed by directly modifying the profiles (Hamarneh et al., 2004). Mesh-based deformable organisms can be simulated as spring-mass systems, allowing deformations to take place through the modification of spring rest-lengths, or the application of forces to the masses or changing their velocities (Hamarneh and McIntosh, 2005). In principle, any shape representation can be used as long as it provides high-level, intuitive deformation control parameters.

15.3.3 Perceptual layer

The perception system of the deformable organism consists of a set of sensors that provide external information to the organisms. Using virtual sensors, an organism can collect data about its environment, such as image data or data from interaction with other organisms. For example, a single organism may have image intensity sensors, edge sensors, and texture sensors. Sensors can be focused or trained for a specific image feature in a task-specific way and, hence, the organism is able to disregard sensory information superfluous to its current behavioral needs.

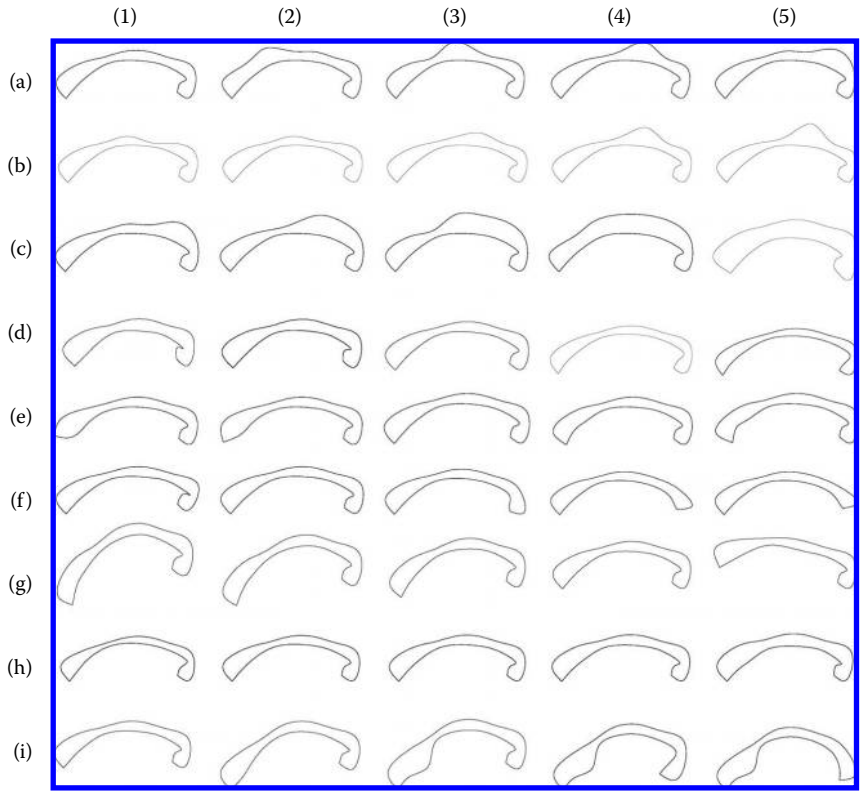

FIGURE 15.4: Examples of controlled deformations: (a)–(c) Operator-based bulge deformation at varying locations/amplitudes/scales. (d) Operator-based stretching with varying amplitudes over entire CC. (e)–(g) Statistics-based bending of left end, right end, and left half of CC. (h) Statistics-based bulge of the left and right thickness over entire CC. (i) From left to right: (1) mean shape, (2) statistics-based bending of left half, followed by (3) locally increasing lower thickness using operator, followed by (4) applying operator-based stretch and (5) adding operator-based bend to right side of CC. (From Hamarneh, G., McInerney, T., Terzopoulos, D. 2001. In *Proceedings of the Medical Image Computing and Computer-Assisted Intervention*, Utrecht, the Netherlands, 66–75. With permission.)

Various parts of the organism are dynamically assigned sensing capabilities and thus act as sensory organs or receptors. A sensor can either be on-board or off-board. On-board sensors are confined to the organisms body, such as at its medial or boundary nodes, at curves or segments connecting different nodes, or at internal geometric subregions, while off-board sensors are free floating. Once the sensory data are gathered, they are fed to the cognitive center of the brain for processing.

A wide variety of image processing techniques can be used to enable the organism to perceive relevant features of its surroundings. In the ITK deformable organisms software framework (Section 15.4.6), the abundant image processing filters supported by the ITK can be applied. The results of potentially complex image processing pipelines can be used as perceptual input to the organisms.

As an example, consider one of the earliest deformable organisms created, the CC worm organism for segmenting the corpus callosum in midsagittal magnetic resonance (MR) images (Section 15.3.4). The geometry-based CC worm is equipped with sensors measuring image intensity, image gradient magnitude and direction, multiscale edge-preserving diffusion-filtered images (Perona and Malik, 1990; Weickert, 1998), a Canny-edge detected version of the image, and the result of a Hough transform applied to locate the top of the human skull in the brain MR image. The physics-based CC deformable organism (Section 15.4.1) was equipped with sensors for collecting statistical measures of image data such as mean and variance, in addition to edge strength and direction sensors. The vessel crawler organisms (Sections 15.2.1 and 15.4.3) used sensory input modules to make decisions about which direction to grow in, and where bifurcations are located. For example, the 2-D angiogram vessel crawler is equipped with an off-board arc sensor (Figure 15.5), which enables it to differentiate between overlapping vessels and authentic branch points. The 3-D crawler makes use of a similar spherical sensor, as well as the eigenvectors of an image intensity-based Hessian (Frangi et al., 1998) to estimate directions of curvature along the vasculature (Figure 15.6).

15.3.4 Behavioral layer

A behavior is defined as the reaction of a life form in response to external or internal stimuli. A deformable organism's behaviors are a set of actions performed in response to perceived input, the actions of other organisms, or input from a user, or they are self-initiated as part of a predetermined plan. Behavioral routines are designed based on the available organism motor skills, perception capabilities, and available anatomical landmarks.

For example, the routines implemented for the CC deformable organism introduced in Hamarneh et al. (2001) include find-top-of-head, find-upper-boundary-of-CC, find-genu, find-rostrum, find-splenium, latch-to-upper-boundary, latch-to-lower-boundary, find-fornix, thicken-right-side, thicken-left-side, and back-up. Each behavior routine subsequently activates the appropriate deformation or growth controllers to complete a stage in the plan and bring an organism closer to its target shape. The progression of these routines is shown in Figure 15.7. Starting from an initial default position shown in subfigure (1), the CC organism goes though different behaviors as it progresses toward its goal. As the upper boundary of the CC is very well defined and can be easily located with respect to the top of the head, the cognitive center of the CC organism activates behaviors to locate first

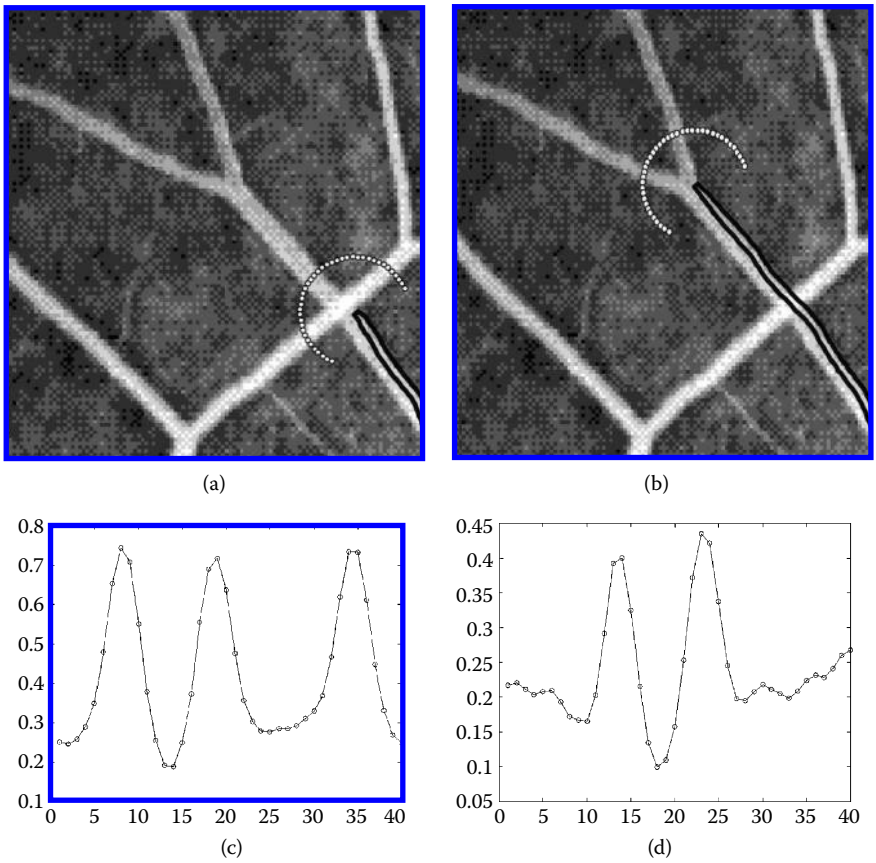

FIGURE 15.5: Off-board sensors (arc of white nodes in (a) and (b)) measure image intensity (along the arc). This results in an intensity profile exhibiting three distinct peaks when an overlapping vessel is ahead (c) and only two peaks in the case of a bifurcation (d).

the top of the head (subfigures 2–3) then move downwards through the gray and white matter in the image space to locate the upper boundary of the CC (4–7). The organism then bends to latch to the upper boundary (8) and activates a find-genu routine, causing the CC organism to stretch and grow along this boundary toward the genu (9–11). It then activates the find-rostrum routine causing the organism to back up, thicken (12), and track the lower boundary until reaching the distinctive rostrum (13–15). Once the rostrum is located, the find-splenium routine is activated and the organism stretches and grows in the other direction (15–16). The genu and splenium are easily detected by looking for a sudden change in direction of the upper boundary toward the middle of the head. At the splenium end of the CC, the organism backs up and finds the center of a circle that approximates

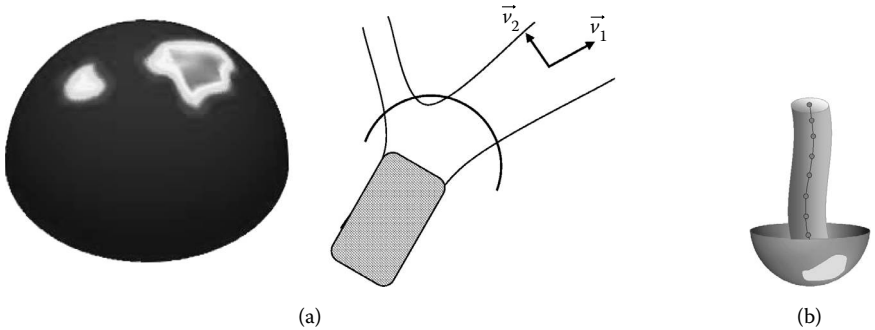

FIGURE 15.6: 3-D sensors for the crawlers. (a) A vessel crawler (gray) utilizing a hemispherical off-board sensor with example output (left), with the primary and secondary eigenvectors of the Hessian computed at optimal scale (top right). (b) A spinal crawler (gray) utilizing a hemispherical "off-board" sensor showing an idealized output (light gray). The crawlers use these sensors to determine the centerline of the vessel/spine tube by extracting the midpoint of the tube's intersection with the surface of the hemisphere. Once the centerline estimate is obtained, the crawlers can add a new layer to their geometry and, consequently, expand along the centerline of the structure (Figures 15.13 and 15.14). (From McIntosh, C., Hamarneh, G. 2006d. *IEEE Conference on Computer Vision and Pattern Recognition*, 1, 1084–1091. With permission.) (From McIntosh, C., Hamarneh, G. 2006c. *Medical Image Computing Analysis and Intervention*, 1, 808–815. With permission.)

the splenium end cap (17). The lower boundary is then progressively tracked from the rostrum to the splenium while maintaining parallelism with the organism's medial axis in order to avoid latching to the potentially connected fornix structure (18–21). Nevertheless, the lower boundary might still dip toward the fornix, so a successive step of locating where, if at all, the fornix connects to the CC is performed by activating the find-fornix routine (making use of edge strength along the lower boundary, its parallelism to the medial axis, and statistical thickness values). Thus, prior knowledge is applied only when and where required. If the fornix is indeed connected to the CC, any detected dip in the organism's boundary is repaired by interpolation using neighboring thickness values. The thickness of the upper boundary is then adjusted to latch to the corresponding boundary in the image (22–26). At this point the boundary of the CC is located (26) and the CC organism has almost reached its goal. However, at this stage the axis is no longer in the middle of the CC organism (27) so it is re-parameterized until the medial nodes are halfway between the boundary nodes (28–30). Finally, the upper and lower boundaries, which were reset in the previous step, are relocated (31–36) to obtain the final segmentation result shown in subfigure (36).

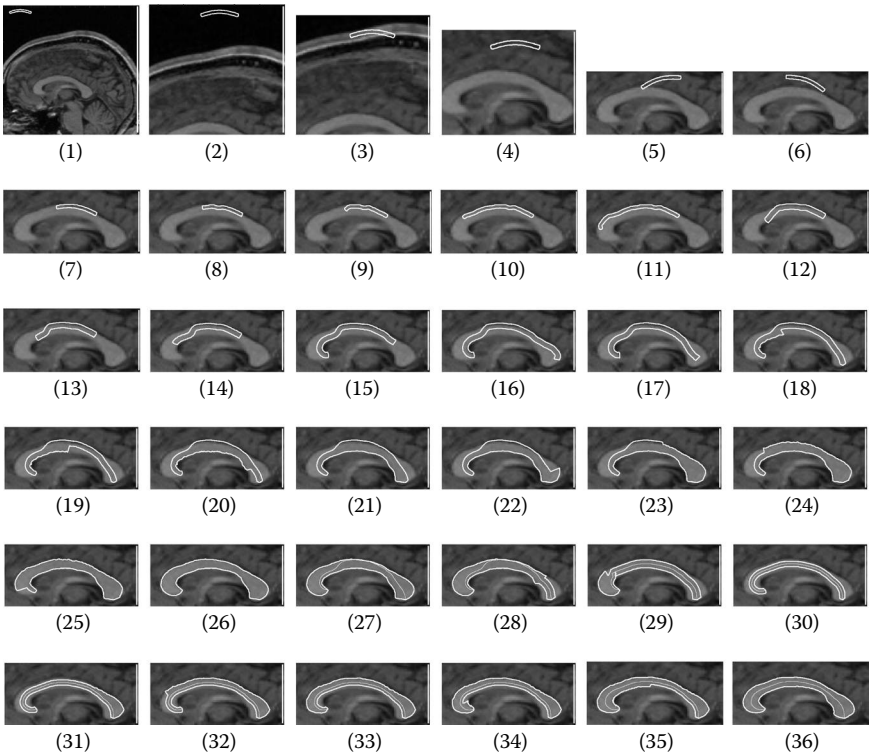

FIGURE 15.7: Deformable corpus callosum organism progressing through a sequence of behaviors to segment the CC (see text). (From McInerney, T., Hamarneh, G., Shenton, M., Terzopoulos, D. 2002. *Medical Image Analysis*, 6(3): 251–266. With permission.)

As a second example, the behaviors exhibited by the physics-based CC deformable organisms (Section 15.4.1) included initializing itself in the image, aligning its body to the CC (first globally, i.e., its whole body, then locally, i.e., its anatomical subregions), and detecting and repairing segmentation inaccuracies commonly caused by the similar image intensity of the fornix.

As a final example, the 3-D vessel crawler (Section 15.4.3) deformable organism included routines for growing or propagating itself along a vessel, fitting or conforming to the vascular boundaries, and spawning new vessel crawlers upon the detection of a branch in the vascular tree.

15.3.5 Cognitive layer

The cognitive layer of the ALife architecture combines memorized information, prior anatomical knowledge, a segmentation plan, and the organism's sensory data (Section 15.3.3) in order to initiate behaviors, carry out shape

deformations, change sensory input, and make decisions toward segmenting and analyzing the target structure (Figure 15.8). A single fixed path in a segmentation plan can be followed, or multiple paths with a plan selection scheme can be implemented. In the first case the organism exhibits a sequential flow of control, proceeding directly from one behavior to the next. In the second case, it decides between different options within the plan, potentially taking different paths given different images or initialization conditions.

Most often, the segmentation plan is subdivided into behavioral stages with subgoals that are easy to define and attain (e.g., locating the upper boundary of an anatomical structure). Consequently, it provides a means for human experts to intuitively incorporate global contextual knowledge. The segmentation plan contains instructions on how best to achieve a correct segmentation by optimally prioritizing behaviors. For example, if it is known that the superior boundary of the CC is consistently and clearly defined in an MR image, then the find-upper-boundary behavior should be given a higher priority as segmenting stable features will provide a good initialization for segmenting nearby less-stable features. Adhering to the segmentation plan and defining it at a behavioral level makes the organism aware of the segmentation process.

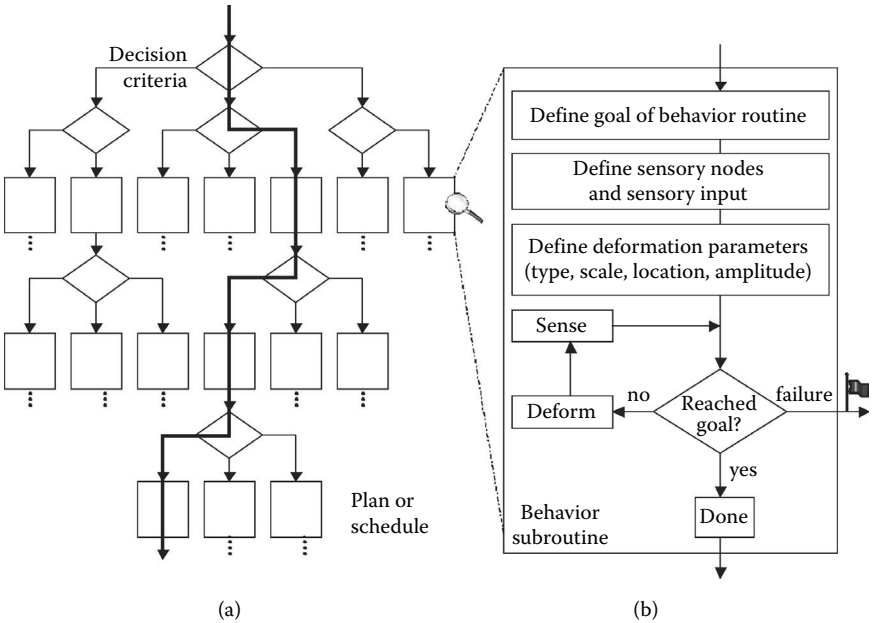

FIGURE 15.8: (a) A procedural representation of a fragment of a deformable organism's plan or schedule. The organism goes through several behavior routines (bold path in a). (b) A simple example of a standard behavior routine. (From McInerney, T., Hamarneh, G., Shenton, M., Terzopoulos, D. 2002. *Medical Image Analysis*, 6(3): 251–266. With permission.)

This enables the organism to make effective use of prior shape knowledge, applying it only in anatomical regions of the target object where a high level of noise or gaps in the objects boundary edge are known to exist.

15.4 Recent Advances

Since its inception in 2001, there have been a number of advances to the original deformable organisms framework. These advances, which are outlined in the following sections, include physical deformation layers, an extension to 3-D, an evolutionary component, and an open-source framework.

15.4.1 Physics-based deformations

A true physical layer was absent in the original work (Hamarneh et al., 2001; McInerney et al., 2002). To complete medical image segmentation tasks, deformable organisms relied on purely geometric shape deformations guided by sensory data, prior structural knowledge, and expert-generated schedules of behaviors. The geometrical deformations made intuitive, real-time user interaction difficult to implement and also necessitated the incorporation of extraneous geometric constraints for maintaining the integrity of the deformable shape model. An early extension to the original deformable organisms framework was to develop and incorporate physics-based shape deformations, which yield additional robustness by enabling intuitive real-time user guidance and interaction when necessary. The physics-based deformations also inherently imposed structural integrity; that is, they provided shape regularization via internal elastic forces.

In Hamarneh and McIntosh (2005), physics-based deformable organisms were presented and applied to the segmentation, labeling, and quantitative analysis of medical image data. External forces are provided by the image gradient and a drag force, while internal forces are supplied through Hookes law and spring damping forces. The results validated that the physics-based formalism allows the expert to provide real-time guidance through small, intuitive interactions, if needed, which further improves the segmentation accuracy and keeps the medical expert "in the loop." Figure 15.9 shows the progression of an example physics-based deformable organism for CC segmentation, Figure 15.10a shows the automatic anatomical labeling, and Figure 15.10b and Figure 15.10c show results before and after some minor user interaction.

15.4.2 Extension to 3-D

A further advancement is the extension of deformable organisms to 3-D for the segmentation and analysis of anatomy in volumetric medical images. To operate in a 3-D environment, deformable organisms need a 3-D geometry that

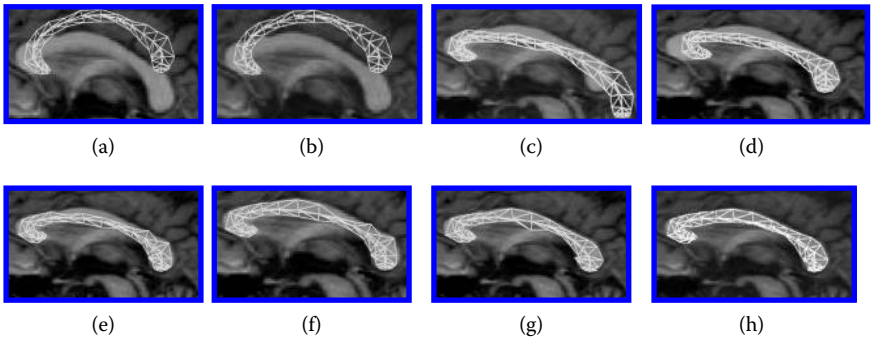

FIGURE 15.9: Progress of segmentation through its primary phases. (a) Global model alignment, (b) model part alignment through (c) expansion and (d) contraction, (e) medial axis alignment, (f) fitting to boundary, (g) detecting and (h) repairing fornix dip. (From Hamarneh, G., McIntosh, C. 2005. In *Proceedings of SPIE Medical Imaging: Image Processing*, 5747, 326–335. With permission.)

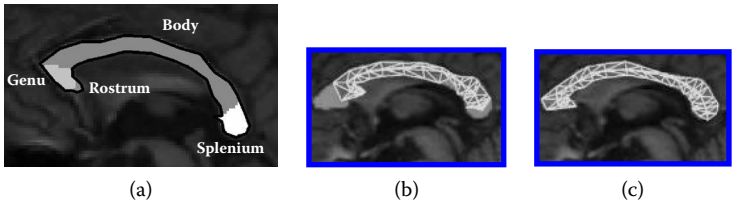

FIGURE 15.10: Physics-based CC organism. (a) Automatic labeling of important anatomical regions of the CC. (b) Before and (c) after intuitive manual intervention to improve the segmentation. (From Hamarneh, G., McIntosh, C. 2005. In *Proceedings of SPIE Medical Imaging: Image Processing*, 5747, 326–335. With permission.)

supports controlled 3-D deformations analogous to the controlled 2-D deformations previously outlined, a 3-D physics layer to carry out those deformations with corresponding behaviors that can operate appropriately in the higher-dimensional environment, 3-D sensors suitable for the 3-D environment, and a cognitive layer that can control the segmentation process. We use medial based shape representation of the organisms 3-D geometry to enable intuitive and localized deformation control, such as medial sheet (Hamarneh et al., 2007) or medial axis based in the case of tubular structures (Sections 15.4.3 and 15.4.4). If physics-based deformations are used (Section 15.4.1) then increasing the dimensionality of the position, force, velocity, and acceleration vectors from 2-D to 3-D enables the calculation of 3-D deformations (Hamarneh and McIntosh, 2005).

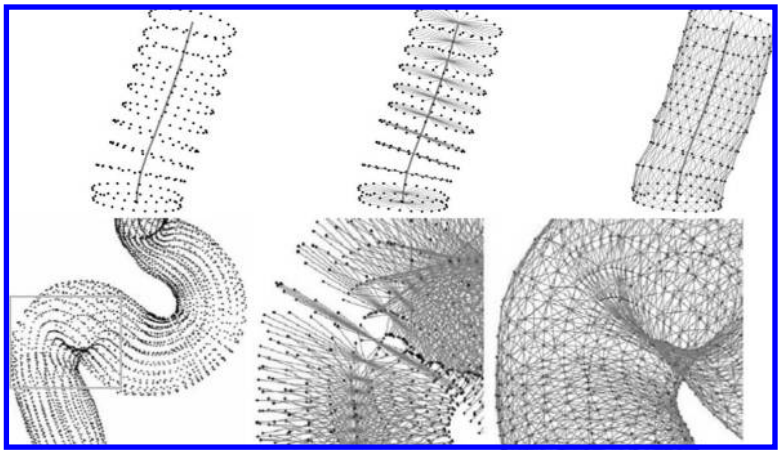

FIGURE 15.11: The geometric and physical layers of tubular shape models. Surface vertices or masses (left) are sampled in a layered fashion along the tubular surface. Radial springs (middle) connect the surface vertices with a medial axis. Stability springs (right) form a triangulated mesh, and act to stabilize the surface model against image noise. (From McIntosh, C., Hamarneh, G. 2006c. *Medical Image Computing Analysis and Intervention*, 1, 808–815. With permission.). (From McIntosh, C., Hamarneh, G. 2006d. *IEEE Conference on Computer Vision and Pattern Recognition*, 1, 1084–1091. With permission.)

The following examples present deformable organisms for the segmentation of tubular structures in volumetric images. The forces are simulated on a tubular geometry parameterized by the distance between neighboring medial masses and the number of circumferential boundary masses (Figure 15.11). This layered medial shape representation enables intuitive deformations (Hamarneh and McInerney, 2003; Hamarneh et al., 2004; O'Donnell, 1994) wherein the medial axis governs the bending and stretching and links to boundary nodes to control thickness. As deformable organisms are typically modeled after their target structures, this tubular branching topology has been employed to the task of vascular and spinal cord segmentation and analysis in volumetric medical images (Sections 15.4.3 and 15.4.4).

15.4.3 Vessel crawlers

In modern internal medicine, noninvasive imaging procedures are often crucial to the diagnosis of cardiovascular, pulmonary, renal, aortic, neurological, and abdominal diseases (Bullitt et al., 2003). Common to the diagnosis of these diseases is the use of volumetric imaging to highlight branching tubular structures such as CT for airways and angiography for vasculature. Without computer assistance, it is difficult to explore, segment, or analyze volumetric images of complex branchings (Figure 15.12).

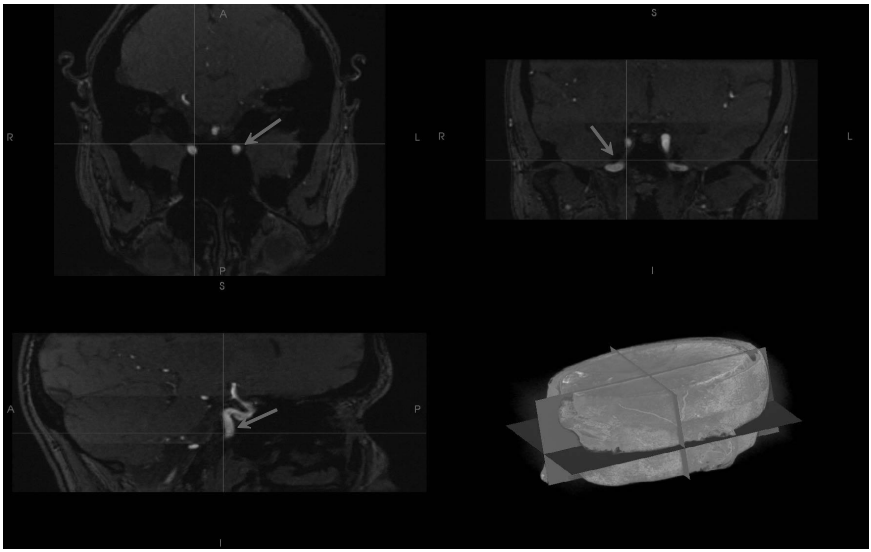

FIGURE 15.12: Slices from a volumetric magnetic resonance angiography image. Plane orientations are shown bottom right. Notice the difficulty in discerning the 3-D structure of the vessels (indicated by the white arrows). Compare this to the segmentations and high-level representations shown in Figures 15.14, 15.15, 15.16, and 15.17. Figure 15.15, for example, gives a quick and intuitive grasp of vessel radius and connectivity.

A new deformable organism for the segmentation and analysis of vasculature from volumetric medical image data was presented in (McIntosh and Hamarneh, 2006d). The bodies of these "vessel crawlers" were modeled as 3-D spring-mass systems (Section 15.4.1). The vessel crawlers use a new repertoire of sensory modules that enable them to detect the centerlines of adjacent vasculature and discern branching points. These sensors are an extension of the arclike sensors in 2-D (Figure 15.5) to a spherical sensor in 3-D (Figure 15.6). They take advantage of optimal vessel filtering, obtained by locally deriving vessel filtering parameters technique (Frangi et al., 1998). Its behavioral routines enable it to grow to the next center-point of a vessel, latch onto the walls of the vessel, and spawn new child vessel crawlers for the exploration of bifurcations in the vascular tree. Finally, a new set of decision-making strategies enables the crawler to decide where to grow to, when to spawn new child vessel crawlers, and when to terminate, all based on its sensory input and current state. Consequently, once initialized within a 3-D image, this new breed of deformable organisms crawls along vasculature, accurately segmenting vessel boundaries, detecting and exploring bifurcations, and providing sophisticated, clinically relevant visualization and structural analysis (Figures 15.13, 15.14, 15.15).

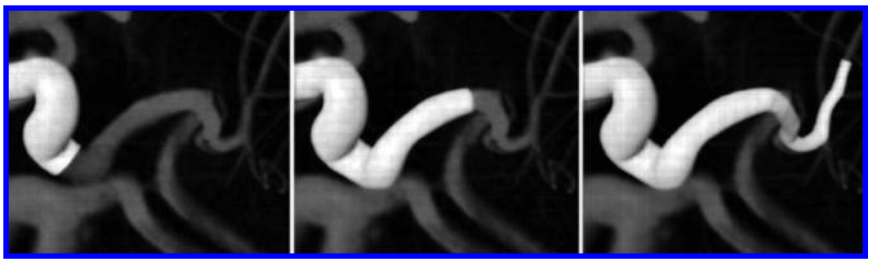

FIGURE 15.13: A 3-D vessel crawler (white arrows) shown as it progressively segments an MRA (shown volume-rendered in grayscale). During each iteration, an estimate of the vessel centerline is obtained from the sensor (Figure 15.6). A new layer is then added with a new medial node at the estimated centerline. Approximately 20 iterations have been performed between each image shown above.

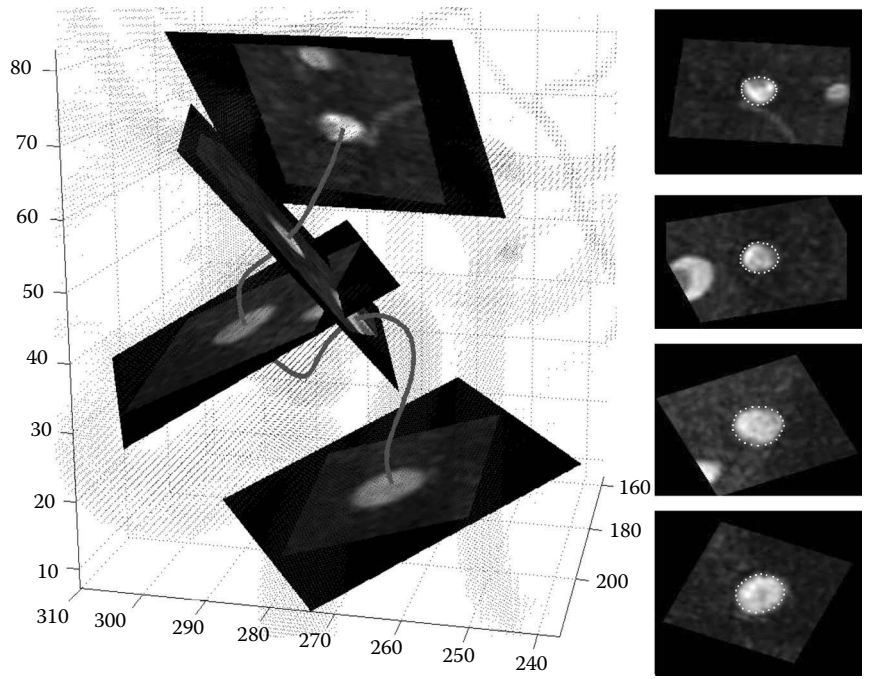

FIGURE 15.14: Multiple cross-sectional slices (left) taken throughout the segmentation process enable the measurement of vessel radii and intensity profiles. Boundary nodes of the vessel crawler after local vessel fitting are shown on extracted slices as white dots (right). (From McIntosh, C., Hamarneh, G. 2006d. *IEEE Conference on Computer Vision and Pattern Recognition*, 1, 1084–1091. With permission.)

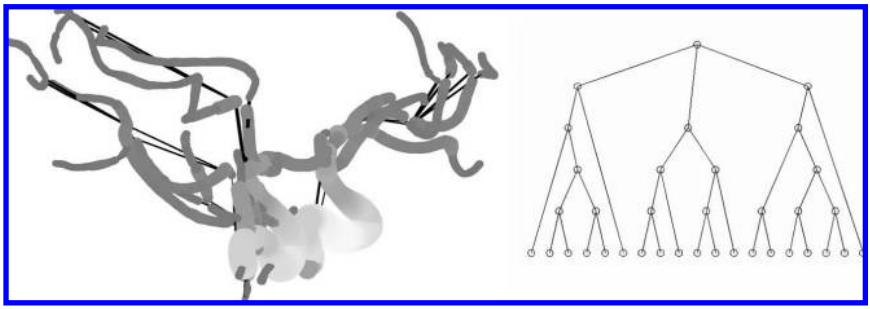

FIGURE 15.15: Intuitive vasculature representations automatically extracted from the MRA image shown in Figure 15.12 (left). Directed acyclic graph (in black) shown in 3-D context overlaid on a plot of the vessels with color corresponding to local radial thickness (right). Tree showing vascular hierarchy displayed out of context. In combination, the two graphs highlight thin vessels (darker gray in the left figure), and give an impression of the overall connectivity (right). Clicking on a node of the tree (right) can also highlight a section of the vasculature (left) along with the set of vessels that feed off of the initial selection. (From McIntosh, C., Hamarneh, G. 2006d. *IEEE Conference on Computer Vision and Pattern Recognition*, 1, 1084–1091. With permission.)

The 3-D vessel crawler extracts clinically relevant features as it crawls though the vasculature, including the distance metric, sum of angles metric, and inflection count metric (Bullitt et al., 2003). In addition to these features, the vessel crawlers are able to label branch points and vessel segments, determine branching angles, cross-sectional radius, vessel segment length, and vessel volume, as well as highlight potential problem areas along with the vascular regions they affect, and the shortest path to those locations from any target point (Figure 15.15) (McIntosh and Hamarneh, 2006d).

For example, the vessel crawler was applied to segment and analyze a computed tomography angiogram (CTA) phantom (Figure 15.16) and a magnetic resonance angiogram (MRA) (Figure 15.17). The vessel crawler was initialized using a single seed point at each of the root vessels. As shown, it was able to detect and track all of the connected vessel segments in the phantom, and the vast majority of connected vessel segments in the MRA.

15.4.4 3-D spinal crawler

The spinal cord is a crucial part of the nervous system that resides within the vertebral canal of the spinal column and acts as a relay to convey information between the brain and the rest of the body. There are numerous clinical problems related to the spinal cord, including multiple sclerosis (MS), meningitis, neural tube defects, syringomyelia, transverse myelitis, and spinal

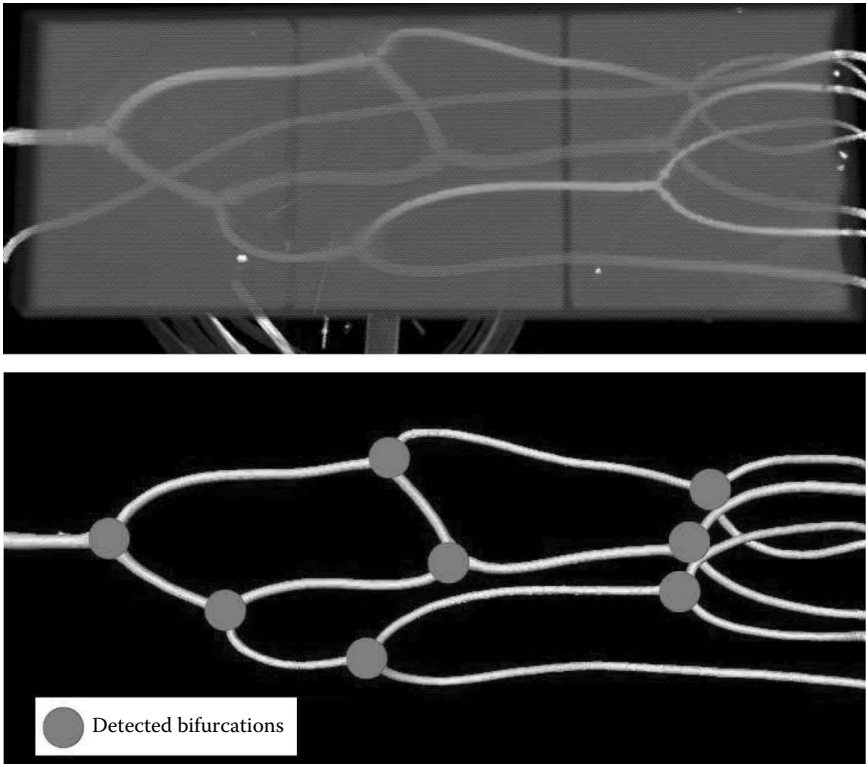

FIGURE 15.16: The figure shows a maximum intensity projection rendering of the phantom CTA (top). We acknowledge Luboz et al. (2005), for providing us with the phantom CTA. Also, it shows the segmentation obtained using vessel crawler (bottom). Notice that the vessel crawler is able to track all the vessels and detect all the bifurcations. (From McIntosh, C., Hamarneh, G. 2006d. *IEEE Conference on Computer Vision and Pattern Recognition*, 1, 1084–1091. With permission.)

cord injury (SCI). MS, for example, which affects more than a quarter million people in the United States, is suspected of shrinking the spinal cord.

To statistically analyze the shape of the spinal cord, a segmentation of the cord must be obtained, which is not a trivial task. Though the cord is approximately cylindrical in shape, its diameter varies at different vertebral levels (Figure 15.18). Furthermore, when progressing from superior to inferior, the spinal cord's information transfer requirement decreases, resulting in decreased white matter and, therefore, decreased contrast. This change in both shape and contrast proves difficult for nonadaptive segmentation and filtering methods. To address this problem, we extended and adapted the vessel crawlers to spinal cord segmentation (McIntosh and Hamarneh, 2006c).

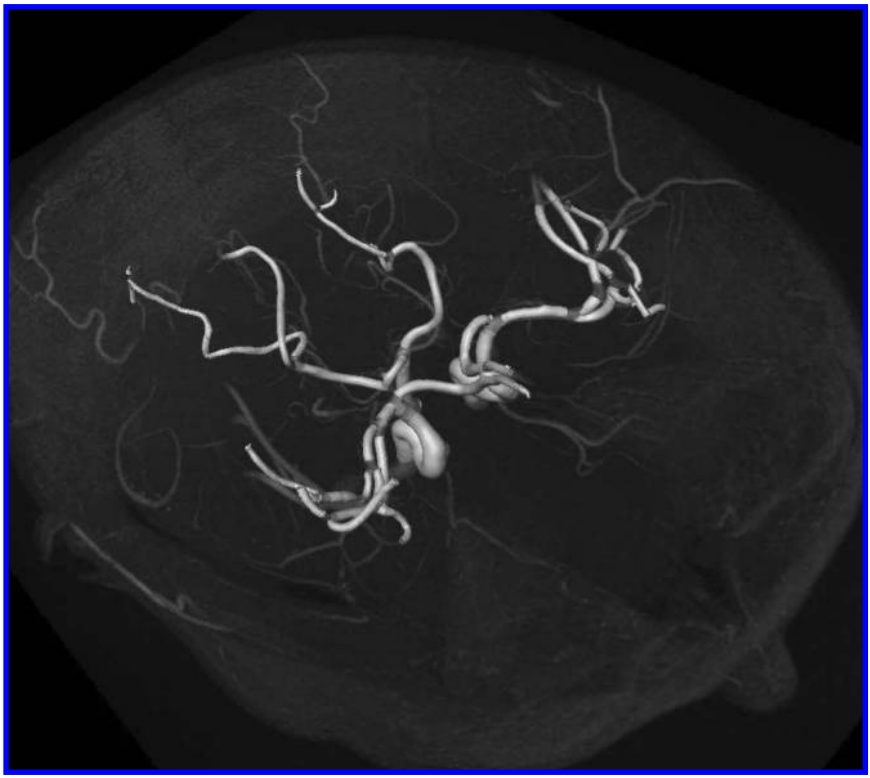

FIGURE 15.17: A volume rendering of a head MRA, viewed superior to inferior (nose appears in the bottom right corner), showing the vessel crawler in shaded white. In this example, the vessel crawler tracks vessel segments with high accuracy, but it fails to detect some of the smaller branch points, resulting in failure to capture the entire tree. (From McIntosh, C., Hamarneh, G. 2006d. *IEEE Conference on Computer Vision and Pattern Recognition*, 1, 1084–1091. With permission.)

The new "spinal crawlers" are tubular spring-mass-based deformable organisms with an adaptive and predominantly elliptical cross section and appropriate anisotropic image data sensors.

By explicitly modeling the elliptical nature of the spinal cord, the spinal crawlers are able to locally detect its shape and intensity characteristics. This information is used to adaptively filter the image, highlighting the spinal cord, and enabling the crawler to perceive the direction in which to grow. The filter extends the single optimal scale in the vessel crawlers with circular cross section (McIntosh and Hamarneh, 2006d) to include two optimal scales, one related to the major axis and the other related to the minor axis of the spinal cord cross section. The result is an anisotropic (elliptical) filter that locally

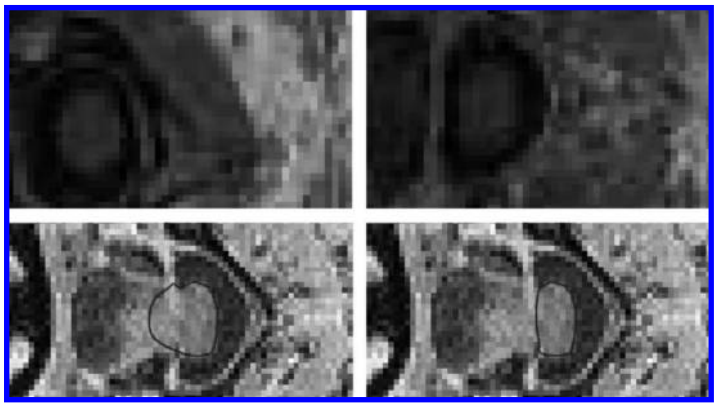

FIGURE 15.18: (See color insert following page 370.) Axial slices of a spinal cord illustrating the difficulty of the segmentation task. Top pair: Circular and elliptical cross-sections of the spinal cord; note the change in shape and lack of contrast. Bottom pair: Extraspinal structures with gray-level intensity higher than that of the spinal cord, which are often encountered in the minor-axis derivatives (horizontal direction). The bottom pair also shows how simple user interaction (Section 15.4.1) on a cross-sectional slice can help repair a false boundary (in red). (From McIntosh, C., Hamarneh, G. 2006c. *Medical Image Computing Analysis and Intervention*, 1, 808–815. With permission.)

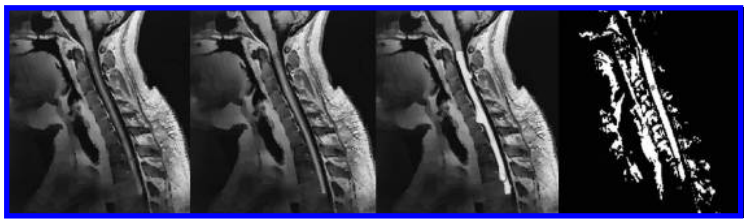

FIGURE 15.19: (See color insert following page 370.) Sample 3-D spinal cord segmentation results (left to right) manual, spinal crawler, SNAP level set, and a region grower with seed point shown in red that has leaked into nearby extraspinal structures. Note that without an adaptive shape prior, SNAP level set (third from the left) frequently leaks outside the spinal cord. (From McIntosh, C., Hamarneh, G. 2006c. *Medical Image Computing Analysis and Intervention*, 1, 808–815. With permission.)

adapts to the spinal cord's shape (as its cross section progresses from elliptical to circular). The results demonstrate the ability of the method to accurately segment the spinal cord, even in areas where popular techniques such as ITK-SNAP (Yushkevich et al., 2006) and region-growing fail (Figure 15.19).

15.4.5 Evolving deformable organisms

A natural extension to the deformable organisms framework is to incorporate evolution. By using algorithms that model natural selection, the organisms can evolve toward improved segmentations of the image data. Specifically, genetic algorithms (GA), a simple survival-of-the-fittest model of evolution, can be employed to evolve a population of shape models where the fitness of a model is measured by how well it segments the image (Ballerini, 1999; McIntosh and Hamarneh, 2006a; MacEachern and Manku, 1998). Consequently, the organisms that produce the best segmentations will be more likely to survive and reproduce, enabling them to pass their parameters on to the next generation. Therefore, over the course of the algorithm, the shape models evolve into an improved segmentation.

For example, the evolution of a population of medial-axis-based CC segmentation organisms was modeled in McIntosh and Hamarneh (2006a). Shape deformations are caused by mutating individual members of the population (Figure 15.20), as well as through crossover (reproduction) operations. Figure 15.21 shows the beginning, middle, and end of the shape model's evolution for two images. The evolution was constrained, and thus the size of the search space reduced, by using statistically based deformable models represented by medial profiles. The deformations are intuitive (stretch, bulge, bend) and driven in terms of the principal modes of variation of a learned mean shape (Figure 15.22) (Hamarneh et al., 2004). Through the simultaneous evolution of a large number of models, the GAs alleviate the typical deformable model weaknesses pertaining to model initialization and energy functional local minima. The results validate that through simulated evolution, the deformable organisms can evolve into states that better segment the target structure than they could through the use of hand-crafted deformation schedules like those in Hamarneh and McIntosh (2005).

15.4.6 Software framework for deformable organisms

Previously, deformable organisms were restricted to a closed-source MATLAB® framework. Though straightforward and intuitive in their design,

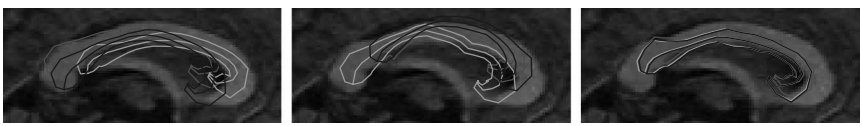

FIGURE 15.20: (See color insert following page 370.) Each image shows evolving deformable organisms whose shape changes result from mutation operators applied sequentially to the medial profiles in order of red, green, blue. Sequential mutations of an increasingly small scale are shown: (a) global scale, (b) medium scale, and (c) small scale.

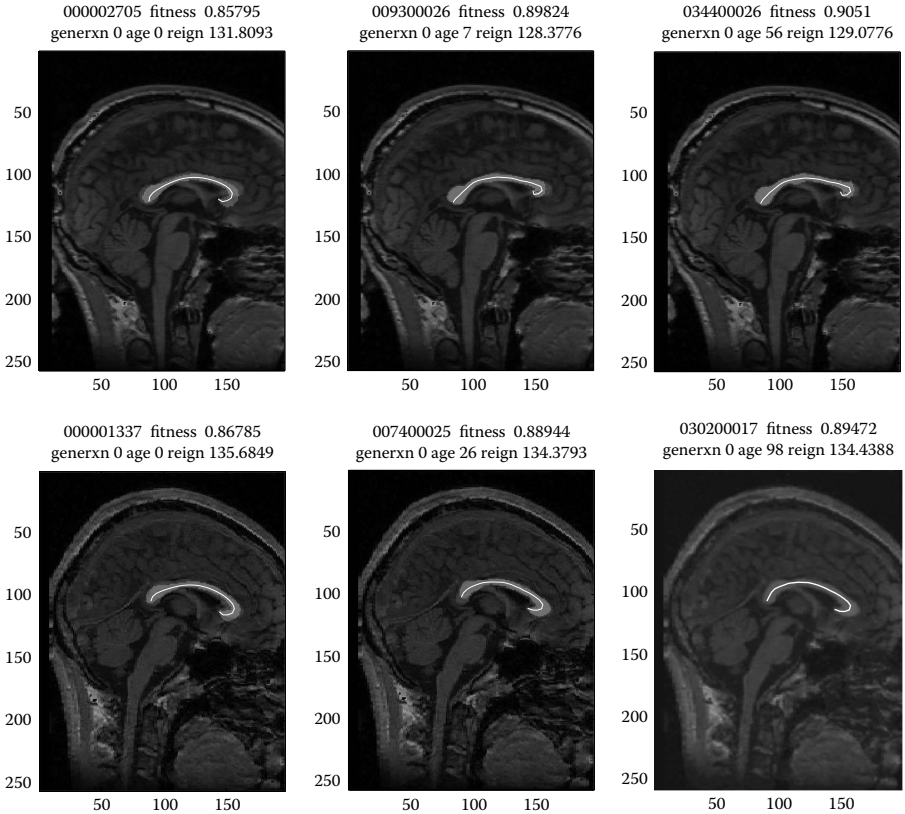

FIGURE 15.21: (See color insert following page 370.) Two example segmentation results progressing left to right, showing the fittest individual after automatic initialization (left), global deformations (middle), and local deformations (right). (From McIntosh, C., Hamarneh, G. 2006a. ACM Workshop on Medical Applications of Genetic and Evolutionary Computation Workshop (MedGEC) in conjunction with the Genetic and Evolutionary Computation Conference (GECCO), 1–8. With permission.)

they were not readily extensible in this form. In McIntosh and Hamarneh (2006b), we reimplemented the deformable organism framework in an open-source manner using the Insight Toolkit (ITK) (www.itk.org), which has a large user base of medical imaging researchers and developers. Furthermore, the incorporation of ITK affords deformable organisms access to faster processing, multithreading, additional image processing functions and libraries, and straightforward compatibility with the powerful visualization capabilities of the Visualization Toolkit (VTK) (www.vtk.org).

Another reason for choosing ITK is because deformable organisms are constructed through the realization of many abstract and independent

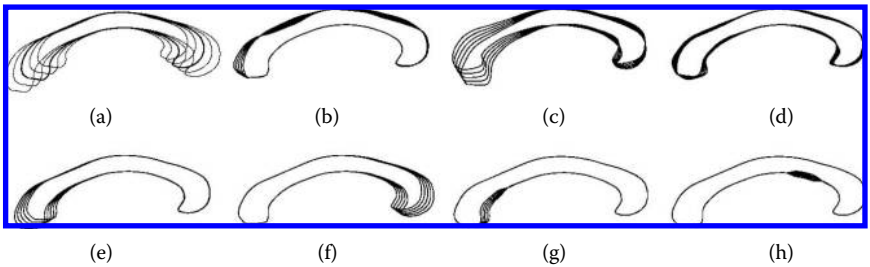

FIGURE 15.22: Statistical shape deformations: (a) global stretch, (b) global upper boundary thickness, (c–d) global bend along two main modes of variation with (c) representing a higher degree of variance, (e–f) localized bend, and (g–h) localized lower boundary thickness for two different scales and locations.

concepts/layers (cognitive, behavioral, physical, geometrical, sensing). Consequently, the deformable organism framework must reflect this modular design by allowing users to replace one implementation (layer) for another. For example, new shape representations should be easily introducible without redesigning existing cognitive layers. To this end, the interface between layers must be clearly defined and consistent across implementations (plug and play).

The software implementation must also be extendable, allowing it to grow and advance as the concept of deformable organisms does. That is, it should support current research into new types of deformable organisms with increasingly advanced decision-making and deformation abilities designed for different applications. These concepts are at the very core of the ITK design methodology.

The ITK Deformable Organisms (I-DO) framework (McIntosh and Hamarneh, 2006b) bridges the ITK framework and coding style with deformable organism design methodologies. It provides a basis for the medical image analysis community to develop new instances of deformable organisms and exchange components (spatial objects, dynamic simulation engines, image sensors, etc.), enabling fast future development of new custom deformable organisms for various clinical applications.

For example, a powerful deformable organism, the itkOrganism, is both a deformable organism and an ITK image filter. Consequently, these organisms can be easily incorporated as autonomous tools into existing ITK filtering pipelines (taking an image as input and producing a segmented image as output). Figure 15.23 demonstrates at a low level the steps required to implement deformable organisms. Although the code excerpts in the figure are specific to the I-DO framework, they represent the general steps we believe need to be taken regardless of the implementation framework or programming language used. The first step is to choose an appropriate shape representation. The

(a)
```
typedef itk::ItkOrganism <ImageType, ImageType, GradientImageType, float, 3> organismType;
organismType::Pointer testOrg = organismType::New();
testOrg->SetInput(reader->GetOutput());
```

(b)
```
typedef Phys_Euler<float,GradientImageType,3> PhysLayerType;
typedef Geom_MeshSpatialObject<float,3> GeometricType;

PhysLayerType::Pointer physLayer = PhysLayerType::New();
GeometricType::Pointer geomLayer = GeometricType::New();
physLayer->setExternalForces((void *) &(output->imageOut));
physLayer->setGeometry(geomLayer);
geomLayer->readTopologyFromFile(topologyInputFileName);
testOrg->setPhysicsLayer(physLayer);
testOrg->setGeometricLayer(geomLayer);
```

(c)
```
Ctrl_ScheduleDriven<float, 3>::Pointer cgL = Ctrl_ScheduleDriven<float, 3>::New();
cgL->setSchedule(scheduleFileName);
testOrg->setCognitiveLayer(cgL);
```

(d)
```
Beh_TranslateAll<float, 3>::Pointer beh1 = Beh_TranslateAll<float,3>::New();
Beh_UniformScale<float, 3>::Pointer beh2 = Beh_UniformScale<float,3>::New();
Def_Translation<float, 3>::Pointer def1 = Def_Translation<float,3>::New();
Def_UniformScale<float, 3>::Pointer def2 = Def_UniformScale<float,3>::New();
testOrg->addBehaviour(beh1);
testOrg->addBehaviour(beh2);
testOrg->addDeformation(def1);
testOrg->addDeformation(def2);
```

(e)
```
testOrg->setRunTime(120);
writer->SetInput(testOrg->GetOutput());
writer->Update();
```

FIGURE 15.23: Example ITK-Deformable Organisms code. Lines are used to (a) initialize the deformable organism, (b) set up and attach the physical and geometrical layers, in this case a spring-mass system, (c) instantiate and attach a cognitive layer, (d) create and attach a set of behaviors and corresponding deformations, and (e) run the deformable organism within an ITK pipeline. (From McIntosh, C., Hamarneh, G., Mori, G. 2007. In *IEEE Workshop on Motion and Video Computing*, 31–38, 2007. With permission.)

issues regarding what constitutes a suitable shape representation for the geometric layer were discussed in Section 15.3.1, most importantly, a shape that provides intuitive deformation handles (code in Figure 15.23b). The second step is to incorporate a method for simulating the deformation dynamics; for example, utilizing mass-spring, physics-based deformations (as discussed in Section 15.3.2; code in Figure 15.23b). The third step is to consult with the domain experts (e.g., clinicians) and identify what constitutes a good strategy for segmentation, thus dictating the sequence of behaviors. As discussed in Section 15.2.5, we recommend progressing from stable to less stable features to improve the robustness of the algorithm (code in Figure 15.23c). The sensors must then be implemented and attached to the deformable organism. The choice of sensors is driven by the goals of the behaviors and the type of features that need to be detected in each behavioral routine (Section 15.3.4). Finally, the different decision-making strategies need to be specified, including

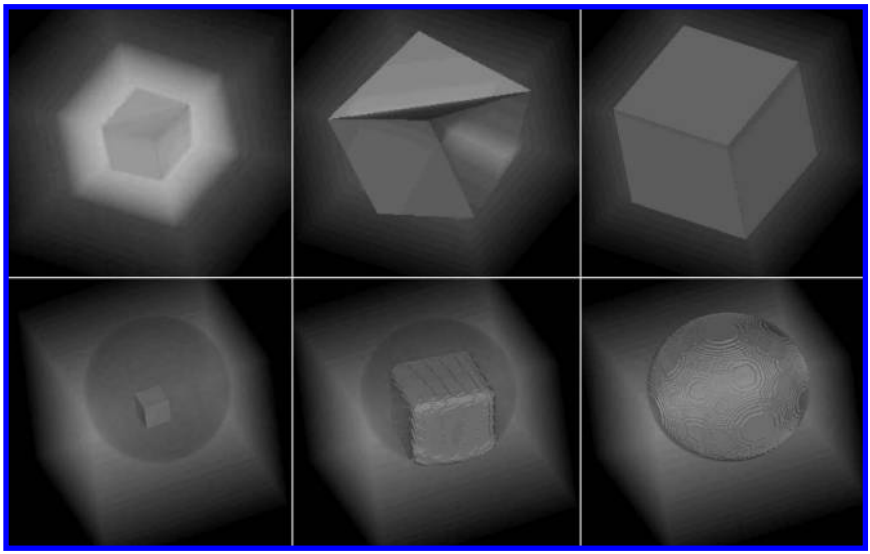

FIGURE 15.24: Two toy example deformable organisms (rendered in gray) progressing from left to right in volume rendered volumetric images. (top) A basic example initialized with a cube, performing a Beh_UniformScale behavior and coming to rest. (bottom) An example initialized with a cube, increasing its size using a Beh_UniformScale behavior simulated on a spring-mass system with the Phys Euler physical layer, then smoothing and coming to rest under image forces using level set–based deformations implemented in the Phys_LevelSet physical layer.

which sensory modules to activate and which behavioral routines to initiate (Section 15.3.5; code in Figure 15.23d).

Other example deformable organisms in the framework can automatically convert between physics-based deformations on spring-mass systems and implicit deformations via the level-sets technique. Two example deformable organisms are shown in Figure 15.24. The bottom row shows a cube is expanded via spring actuation, then automatically converted to a level-set representation and deformed using image gradients.

15.5 Discussion

The original ideas of deformable organisms were presented in Hamarneh, McInerney, and Terzopoulos (2001), Hamarneh (2001), and McInerney et al. (2002). In this original research, several examples of deformable organisms for segmenting and labeling anatomy from medical images were demonstrated.

The classical example is the CC deformable organism, also affectionately referred to as the *CC worm*, which was developed to segment the corpus callosum (CC) in midsagittal brain MR images. The underlying geometry and shape deformations (medial profiles), several of its behavioral routines (e.g., bending, stretching and thickening to crawl and latch to boundaries), and perception capabilities (e.g., edge-detectors) were reused to create interacting organisms (ventricles, putamen, and caudate nucleus) and then 2-D vessel crawlers that detect branches and spawn new child organisms.

As we discussed in the previous section, several extensions have been developed in recent years, from physics-based deformations to 3-D vessel and spinal crawlers to evolutionary organisms to the I-DO ITK-software framework for deformable organisms.

The deformable organisms framework provides several advantages not seen together in any other medical image analysis technique or class of techniques. These advantages include a design that bridges the gap between contextual knowledge and low-level image processing, a layered, modular framework that allows for component reuse and rapid building of new custom medical image analysis applications, a built-in consciousness exemplified by the organisms' awareness of the part of anatomy they are targeting to delineate or label at the current stage of the segmentation plan, the ability to incorporate human input either through user interaction or prestored expert knowledge, and the ability to flag a difficulty or failure should it arise.

15.6 Future Research Directions

Research into the ALife deformable organisms framework is by no means complete. Many improvements can be made in each of the layers, including improved shape representation and deformation capabilities, improved simulation of deformation dynamics, improved design of plans and strategies for medical image analysis, improved incorporation of domain knowledge, and the adoption of improved image processing algorithms used for the organisms' sensory input. Most importantly, all these extensions will be most meaningful if they are applied to practical, clinically motivated medical image analysis applications.

Our existing deformable organisms have been restricted to static 2-D or 3-D images. An important area for future research is dynamic deformable organisms that can analyze motion in time-varying medical imagery. Like conventional deformable models, deformable organisms can be extended to dynamic deformable organisms capable of tracking moving objects in spatiotemporal image data. In McIntosh, Hamarneh, and Mori (2007), we presented a dynamic deformable organism for tracking walking humans from color video (sequences of 2-D color images). The geometry of this "human tracker" deformable organism is a multifigural medial representation, where the torso

and each limb is based on a medial-axis description and the inter-limb connectivity follows the articulated human structure (wrist to elbow, elbow to shoulder, etc.). Using appropriate sensors and behaviors (deformation control sequences), the organisms can search for the person appearing in each frame and automatically delineate his or her boundaries and joint positions. Results are presented in McIntosh and others (2007). Dynamic deformable organisms along these lines remain to be developed for time-varying 2-D and 3-D medical image analysis.

15.7 Conclusions

In this chapter, we reviewed deformable organisms, a novel paradigm for highly automated medical image analysis. The deformable organisms framework is based on deformable models augmented by ALife modeling concepts. This is realized through the knowledge-based, top-down modeling of cognitive, perceptual, and behavioral processes that control and guide the common low-level, bottom-up, data-driven deformable models technique. The result is novel image analysis algorithms that incorporate high-level models of how medical experts approach a medical image analysis task.

Deformable organisms are autonomous agents that can automatically segment, label, and quantitatively analyze anatomical structures of interest in medical images. Rather than relying on expert human interaction to initialize deformable models, set their free parameters, and guide their evolution in order to attain accurate segmentations, deformable organisms incorporate an intelligent, artificial brain that automatically performs these tasks with excellent results. This chapter motivated and overviewed deformable organisms, explained the principal layers of their ALife modeling architecture, reviewed some of the original deformable organism instances, outlined recent extensions and advances, and suggested avenues for future research relevant to this promising new medical image analysis technique.

References

Attali, D., Montanvert, A. 1997. Computing and simplifying 2D and 3D continuous skeletons. *Computer Vision and Image Understanding* 67(3), 261–273.

Ballerini, L. 1999. Genetic snakes for medical images segmentation. In R. Poli, Ed., *Evolutionary Image Analysis, Signal Processing and Telecommunications.* Berlin, Springer, pp. 59–73.

Barr, A. 1984. Global and local deformations of solid primitives. In *Proceedings of the 11th Annual Conference on Computer Graphics and Interactive Techniques (SIGGRAPH84)* 18, New York, 21–30.

Blum, H. 1973. Biological shape and visual science. *Theory of Biology* 38, 205–287.

Bookstein, F. 1997. *Morphometric Tools for Landmark Data: Geometry and Biology*. Cambridge: Cambridge University Press.

Borgefors, G., Nystrom, I., Baja, G. S. D. 1999. Computing skeletons in three dimensions. *Pattern Recognition* 32, 1225–1236.

Bouix, S., Dimitrov, P., Phillips, C., Siddiqi, K. 2000. Physics-based skeletons. In *Proceedings of the Vision Interface Conference*, 23–30.

Bullitt, E., Gerig, G., Aylward, S. R., Joshi, S. C., Smith, K., Ewend, M., Lin, W. 2003. Vascular attributes and malignant brain tumors. In *Proceedings of the Sixth International Conference on Medical Image Computing and Computer-Assisted Intervention (MICCAI03). Lecture Notes in Computer Science* 2878, Springer, Berlin, 671–679.

Burel, G., Henocq, H. 1995. Three-dimensional invariants and their application to object recognition. *Signal Process* 45(1), 1–22.

Cootes, T. F., Beeston, C., Edwards, G., Taylor, C. 1999. A unified framework for atlas matching using active appearance models. In *Proceedings of the Image Processing in Medical Imaging Conference*, Visegrad, Hungary, 322–333.

Cootes, T. F., Cooper, D., Taylor, C. J., Graham, J. 1995. Active shape models: their training and application. *Computer Vision and Image Understanding* 61(1), 38–59.

Cootes, T. F., Edwards, G. J., Taylor, C. J. 2001. Active appearance models. *IEEE Transactions on Pattern Analysis and Machine Intelligence* 23(1), 681–685.

Coquillart, S. 1990. Extended free form deformations: a sculpting tool for 3D geometric modeling. In *Proceedings of the 17th Annual Conference on Computer Graphics and Interactive Techniques (SIGGRAPH90)* 24, New York, 187–196.

Costa, L., Cesar, Jr R. 2000. *Shape Analysis and Classification: Theory and Practice*. Boca Raton, FL: CRC Press.

Davatzikos, C., Tao, X., Shen, D. 2003. Hierarchical active shape models: using the wavelet transform. *IEEE Transactions on Medical Imaging* 22(3), 414–423.

Dimitrov, P., Damon, J., Siddiqi, K. 2003. Flux invariants for shape. In *Proceedings of the IEEE Computer Society Conference on Computer Vision and Pattern Recognition (CVPR03)*, Washington, DC, 835–841.

Dryden, I., Mardia, K. 1998. *Statistical Shape Analysis*. New York: Wiley.

Duncan, J., Ayache, N. 2000. Medical image analysis: Progress over two decades and the challenges ahead. *IEEE Transactions on Pattern Analysis and Machine Intelligence* 22(1), 85–106.

Duta, N., Sonka, M., Jain, A. 1999. Learning shape models from examples using automatic shape clustering and Procrustean analysis. In *Proceedings of the 17th International Conference on Information Processing in Medical Imaging (IPMI99). Lecture Notes in Computer Science* 1613, Springer, Berlin, 370–375.

Fletcher, P., Conglin, L., Pizer, S., Joshi, S. 2004. Principal geodesic analysis for the study of nonlinear statistics of shape. *IEEE Transactions on Medical Imaging* 23(8), 995–1005.

Frangi, A. F., Niessen, W. J., Vincken, K. L., Viergever, M. A. 1998. Multiscale vessel enhancement filtering. *Lecture Notes in Computer Science* 1496, 130–137.

Fritsch, D., Pizer, S., Yu, L., Johnson, V., Chaney, E. 1997. Segmentation of medical image objects using deformable shape loci. In *Proceedings of the 15th International Conference on Information Processing in Medical Imaging (IPMI97). Lecture Notes in Computer Science* 1230, Springer, Berlin, 127–140.

Grenander, U. 1963. *Probabilities on Algebraic Structures*. New York: Wiley.

Hamarneh, G. 2001. Toward Intelligent Deformable Models for Medical Image Analysis. Ph.D. Thesis, Chalmers University of Technology, Göteborg, Sweden.

Hamarneh, G., McInerney, T. 2003. Physics-based shape deformations for medical image analysis. In *Proceedings of the 2nd SPIE Conference on Image Processing: Algorithms and Systems (SPIEIST 03)* 5014, 354–362.

Hamarneh, G., McIntosh, C. 2005. Physics-based deformable organisms for medical image analysis. In *Proceedings of SPIE Medical Imaging: Image Processing* 5747, 326–335.

Hamarneh, G., McInerney, T., Terzopoulos, D. 2001. Deformable organisms for automatic medical image analysis. In *Proceedings of the Medical Image Computing and Computer-Assisted Intervention*, Utrecht, the Netherlands, 66–75.

Hamarneh, G., Abu-Gharbieh, R., McInerney, T. 2004. Medial profiles for modeling deformation and statistical analysis of shape and their use in medical image segmentation. *International Journal of Shape Modeling* 10(2), 187–209.

Hamarneh, G., Ward, A., and Frank, R. 2007. Quantification and visualization of localized and intuitive shape variability using a novel medial-based shape representation. In *IEEE International Symposium on Biomedical Imaging (ISBI)*.

Kass, M., Witkin, A., Terzopoulos, D. 1988. Snakes: active contour models. *International Journal of Computer Vision* 1(4), 321–331.

Lachaud, J., Montanvert, A. 1999. Deformable meshes with automated topology changes for coarse-to-fine three-dimensional surface extraction. *Medical Image Analysis* 3(1), 1–21.

Leventon, M., Grimson, W., Faugeras, O. 2000. Statistical shape influence in geodesic active contours. In *Proceedings of the IEEE Computer Society Conference on Computer Vision and Pattern Recognition* 1, Washington, DC, 316–323.

Levy, S. *Artificial Life*. New York: Pantheon, 1992.

Leymarie, F., Levine, M. D. 1992. Simulating the grassfire transform using an active contour model. *IEEE Transactions on Pattern Analysis and Machine Intelligence* 14(1), 56–75.

Lu, C., Pizer, S., Joshi, S. 2003. A Markov random field approach to multiscale shape analysis. In *Proceedings of the Conference on Scale Space Methods in Computer Vision. Lecture Notes in Computer Science* 2695, Springer, Berlin, 416–431.

Luboz, V., Wu. X., Krissian, K., Westin, C.-F., Kikinis. R., Cotin, S., Dawson. S. A segment and reconstraction technique for 3D vascular structures. In MICCS, 2005, 43–50. Palm Springs, CA.

MacEachern L., Manku T. 1998. Genetic algorithms for active contour optimization. *IEEE Proceedings of the International Symposium on Circuits and Systems* 4, 229–232.

Mandal, C., Vemuri, B., Qin, H. 1998. A new dynamic FEM-based subdivision surface model for shape recovery and tracking in medical images. In *Proceedings of the First International Conference on Medical Image Computing and Computer-Assisted Intervention (MICCAI98). Lecture Notes in Computer Science* 1496, Springer, Berlin, 753–760.

McInerney, T., Kikinis, R. 1998. An object-based volumetric deformable atlas for the improved localization of neuroanatomy in MR images. In *Proceedings of the Medical Image Computing and Computer-Assisted Intervention*, Cambridge, MA, 861–869.

McInerney, T., Terzopoulos, D. 1995. A dynamic finite-element surface model for segmentation and tracking in multidimensional medical images with application to cardiac 4D image analysis. *Computerized Medical Imaging and Graphics* 19(1), 69–83.

McInerney, T., Terzopoulos, D. 1996. Deformable models in medical image analysis: a survey. *Medical Image Analysis* 1(2), 91–108.

McInerney, T., Hamarneh, G., Shenton, M., Terzopoulos, D. 2002. Deformable organisms for automatic medical image analysis. *Medical Image Analysis* 6(3), 251–266.

McIntosh, C., Hamarneh, G. 2006a. Genetic algorithm driven statistically deformed models for medical image segmentation. ACM Workshop on Medical Applications of Genetic and Evolutionary Computation Workshop (MedGEC) in conjunction with the Genetic and Evolutionary Computation Conference (GECCO), 1–8.

McIntosh, C., Hamarneh, G. 2006b. I-DO: A Deformable Organisms Framework for ITK. Medical Image Computing Analysis and Intervention Open Science Workshop 2006, 1–14.

McIntosh, C., Hamarneh, G. 2006c. Spinal crawlers: deformable organisms for spinal cord segmentation and analysis. *Medical Image Computing Analysis and Intervention* (1), 808–815.

McIntosh, C., Hamarneh, G. 2006d. Vessel crawlers: 3D physically-based deformable organisms for vasculature segmentation and analysis. *IEEE Conference on Computer Vision and Pattern Recognition* 1, 1084–1091.

McIntosh, C., Hamarneh, G., Mori, G. 2007. Human limb delineation and joint position recovery using localized boundary models. In *IEEE Workshop on Motion and Video Computing*, 31–38, 2007.

Miller, J., Breen, D., Lorensen, W., O'Bara, R., Wozny, M. J. 1991. Geometrically deformed models: a method for extracting closed geometric models from volume data. In *Proceedings of the 18th Annual Conference on Computer Graphics and Interactive Techniques (SIGGRAPH91)* 25, New York, 217–226.

Montagnat, J., Delingette, H. 1997. Volumetric medical image segmentation using shape constrained deformable models. In *Proceedings of the Second International Conference on Computer Vision, Virtual Reality and Robotics in Medicine (CVRMed-MRCAS97). Lecture Notes in Computer Science* 1205, Springer, Berlin, 13–22.

Mortenson, M. 1997. *Geometric Modeling*. New York: Wiley.

O'Donnell, T., Boult, T., Fang, X., Gupta, A. 1994. The extruded generalized cylinder: a deformable model for object recovery. In *Proceedings of the IEEE Computer Society Conference on Computer Vision and Pattern Recognition (CVPR94)*, Washington, DC, 174–181.

Perona, P., Malik, J. 1990. Scale-space and edge detection using anisotropic diffusion. *IEEE Transactions on Pattern Analysis and Machine Intelligence* 12(7), 629–639.

Pizer, S., Fritsch, D. 1999. Segmentation, registration, and measurement of shape variation via image object shape. *IEEE Transactions on Medical Imaging* 18(10), 851–865.

Pizer, S., Gerig, G., Joshi, S., Aylward, S. R. 2003. Multiscale medial shape-based analysis of image objects. In *Proceedings of IEEE* 91(10), 1670–1679.

Sebastian, T., Klein, P., Kimia, B. 2001. Recognition of shapes by editing shock graphs. In *Proceedings of the International Conference on Computer Vision (ICCV01)*, Washington, DC, 755–762.

Sederberg, T. W., Parry, S. R. 1986. Free-form deformation of solid geometric models. In *Proceedings of the 13th Annual Conference on Computer Graphics and Interactive Techniques (SIGGRAPH86)* 4, New York, 151–160.

Shen, D., Davatzikos, C. 2000. An adaptive-focus deformable model using statistical and geometric information. *IEEE Transactions on Pattern Analysis and Machine Intelligence* 22(8), 906–913.

Siddiqi, K., Bouix, S., Tannenbaum, A., Zucker, S. 2002. Hamilton-Jacobi skeletons. *International Journal of Computer Vision* 48(3), 215–231.

Singh, K., Fiume, E. 1998. Wires: A geometric deformation technique. In *Proceedings of the 25th Annual Conference on Computer Graphics and Interactive Techniques (SIGGRAPH98)* 99(1), New York, 405–414.

Styner, M., Gerig, G., Lieberman, J., Jones, D., Weinberger, D. 2003. Statistical shape analysis of neuroanatomical structures based on medial models. *Medical Image Analysis* 7(3), 207–220.

Szekely, G., Kelemen, A., Brechbuehler, C. H., Gerig, G. 1996. Segmentation of 3D objects from MRI volume data using constrained elastic deformations of flexible Fourier surface models. *Medical Image Analysis* 1(1), 19–34.

Terzopoulos, D., Metaxas, D. 1991. Dynamic 3D models with local and global deformations: Deformable superquadrics. *IEEE Transactions on Pattern Analysis and Machine Intelligence* 13(7), 703–714.

Terzopoulos, D., Tu, X., Grzeszczuk, R. 1994. Artificial fishes: autonomous locomotion, perception, behavior, and learning in a simulated physical world. *Artificial Life* 1(4), 327–351.

Terzopoulos, D. 1999. Artificial life for computer graphics. *Communications of the ACM* 42(8), 32–42.

Tsotsos, J., Mylopoulos, J., Covvey, H. D., Zucker, S. W. 1980. A framework for visual motion understanding. *IEEE Transactions on Pattern Analysis and Machine Intelligence* 2(6), 563–573.

Ullman, S. 1984. Visual routines. *Cognition* 18, 97–159.

Weickert, J. 1998. *Anisotropic Diffusion in Image Processing*. ECMI Series. Stuttgart: Teubner.

Yushkevich, P., Joshi, S., Pizer, S. M., Csernansky, J., Wang, L. 2003. Feature selection for shape-based classification of biological objects. In *Proceedings of the 17th International Conference on Information Processing in Medical Imaging (IPMI03). Lecture Notes in Computer Science* 2732, Springer, Berlin, 114–125.

Yushkevich, P. A., Piven, J., Hazlett, H. C., Smith, R. G., Ho, S., Gee, J. C., Gerig, G. 2006. User-guided 3D active contour segmentation of anatomical structures: Significantly improved efficiency and reliability. *Neuroimage*.